Deep-Sea Research II 56 (2009) 2822–2838

Contents lists available at ScienceDirect

Deep-Sea Research II

journal homepage: www.elsevier.com/locate/dsr2

Behaviors of dissolved and particulate Co, Ni, Cu, Zn, Cd and Pb during a mesoscale Fe-enrichment experiment (SEEDS II) in the western North Pacific

Seiji Nakatsuka [a,*], Kei Okamura [b], Shigenobu Takeda [c], Jun Nishioka [d], M. Lutfi Firdaus [a], Kazuhiro Norisuye [a], Yoshiki Sohrin [a]

[a] Institute for Chemical Research, Kyoto University, Uji, Kyoto 611-0011, Japan
[b] Center for Advanced Marine Core Research, Kochi University, Monobe, Nankoku, Kochi 783-8502, Japan
[c] Graduate School of Agricultural and Life Sciences, The University of Tokyo, Yayoi, Bunkyo-ku, Tokyo 113-8657, Japan
[d] Institute of Low temperature Science, Hokkaido University, Sapporo, Hokkaido 060-0819, Japan

ARTICLE INFO

Topical issue on "SEEDS II: The Second Subarctic Pacific Iron Experiment for Ecosystem Dynamics Study." The issue is compiled and guest-edited by the North Pacific Marine Science Organization (PICES) and International SOLAS.
Available online 3 July 2009

Keywords:
Western North Pacific Ocean
Seawater
Trace metal
SEEDS II
Mesoscale Fe enrichment
Shipboard bottle incubation

ABSTRACT

During mesoscale Fe enrichment (SEEDS II) in the western North Pacific ocean, we investigated dissolved and particulate Co, Ni, Cu, Zn, Cd and Pb in seawater from both field observation and shipboard bottle incubation of a natural phytoplankton assemblage with Fe addition. Before the Fe enrichment, strong correlations between dissolved trace metals (Ni, Zn and Cd) and PO_4^{3-}, and between particulate trace metals (Ni, Zn and Cd) and chlorophyll-*a* were obtained, suggesting that biogeochemical cycles mainly control the distributions of Ni, Zn and Cd in the study area. Average concentrations of dissolved Co, Ni, Cu, Zn, Cd and Pb in the surface mixed layer (0–20 m) were 70 pM, 4.9, 2.1, 1.6, 0.48 nM and 52 pM, respectively, and those for the particulate species were 1.7 pM, 0.052, 0.094, 0.46, 0.037 nM and 5.2 pM, respectively. After Fe enrichment, chlorophyll-*a* increased 3 fold (up to 3 $\mu g\,L^{-1}$) during developing phases of the bloom (<12 days). Mesozooplankton biomass also increased. Particulate Co, Ni, Cu and Cd inside the patch hinted at an increase in the concentrations, but there were no analytically significant differences between concentrations inside and outside the patch. The bottle incubation with Fe addition (1 nM) showed an increase in chlorophyll-*a* (8.9 $\mu g\,L^{-1}$) and raised the particulate fraction up to 3–45% for all the metals, accompanying changes in Si/P, Zn/P and Cd/P. These results suggest that Fe addition lead to changes in biogeochemical cycling of trace metals. The comparison between the mesoscale Fe enrichment and the bottle incubation experiment suggests that although Fe was a limiting factor for the growth of phytoplankton, the enhanced biomass of mesozooplankton also limited the growth of phytoplankton and the transformation of trace metal speciation during the mesoscale Fe enrichment. Sediment trap data and the elemental ratios taken up by phytoplankton suggest that export loss was another reason that no detectable change in the concentrations of particulate trace metals was observed during the mesoscale Fe enrichment.

1. Introduction

The subarctic North Pacific, equatorial Pacific and Southern Oceans are classified into high-nitrate low-chlorophyll (HNLC) regions, where Fe has been suggested as a prime micronutrient controlling the growth and biomass of phytoplankton. This finding was confirmed by mesoscale Fe enrichments in these regions (Coale et al., 1996, 2004; Martin et al., 1994; Tsuda et al., 2003).

In addition to Fe, various trace metals are essential to marine organisms, often as co-factors in enzymes and as structural elements in biomolecules (Morel and Price, 2003). Co is well known as a central metal in a corrin ring core of vitamin B_{12} and is an essential micronutrient for *Prochlorococcus* (Saito et al., 2002). Ni is a co-factor in urease. Cu is a co-factor in Cytochrome *c* oxidase (da Silva and Williams, 2001), and in enzymes, such as multicopper oxidase (La Fontaine et al., 2002), and proteins, such as plastocyanin (Peers and Price, 2006), recently identified to be important in eukaryotic phytoplankton. Zn is present in a large number of enzymes including alkaline phosphatase and carbonic anhydrase (Morel and Price, 2003). Cd is also contained in Cd-specific carbonic anhydrase in diatom *Thalassiosira weissflogii* (Cullen et al., 1999; Lane et al., 2005). It is also suggested that substitution of an essential metal for another is common in marine phytoplankton (Morel and Price, 2003). Moreover, recent studies suggest that Fe availability is likely to affect the elemental stoichiometry of Co, Ni, Zn and Cd in phytoplankton (Cullen et al., 2003; Twining et al., 2004).

* Corresponding author. Tel.: +81 774 38 3097; fax: +81 774 38 3099.
E-mail address: nakatuka@inter3.kuicr.kyoto-u.ac.jp (S. Nakatsuka).

0967-0645/$ - see front matter © 2009 Elsevier Ltd. All rights reserved.
doi:10.1016/j.dsr2.2009.06.008

Biogeochemical cycles are thought to be a major factor controlling the distribution and partition of dissolved and particulate trace metals in seawater. However, it is difficult to observe directly the effect of biological activities on the distribution and partition of trace metals, especially in the open sea. Recently, some data have been reported on the interaction between organisms and trace metals during the mesoscale Fe-enrichment experiments (Gordon et al., 1998; Frew et al., 2001; Kinugasa et al., 2005). The results were very different among the experiments. The concentrations of dissolved and particulate trace metals (Al, Cd, Co, Cu, Mn, Ni and Zn) did not change significantly during IronEx I in the eastern equatorial Pacific Ocean (Gordon et al., 1998). During SOIREE in the Southern Ocean, there were no significant variations for dissolved Ni, Cu and Zn concentrations, while 70% of initial dissolved Cd was partitioned into particulate matter due to biological utilization by algae (Frew et al., 2001). In contrast, Kinugasa et al. (2005) found significant decreases in dissolved concentrations of Co, Ni, Cu, Zn and Cd during SEEDS I in the western North Pacific. They suggested that the dissolved trace metals were taken up by algae and incorporated into particulate species. According to their dissolved and acid-dissolvable data, the particulate trace metals remained in the mixed layer during SEEDS I. These mesoscale Fe enrichments mainly focused on the development phase of the bloom over less than 13 days.

The second Fe-enrichment experiment in the western North Pacific (SEEDS II) was carried out in summer 2004 (Tsuda et al., 2007). We observed variations in dissolved and particulate Co, Ni, Cu, Zn, Cd and Pb inside and outside the Fe patch for 26 days to cover the developing and declining phases of the bloom. We also conducted bottle incubation experiments with Fe addition on board the vessel using surface seawater, from which mesozooplankton had been removed, and followed the changes in trace metals. We report different behaviors of the trace metals between the mesoscale Fe enrichment and the bottle incubation experiments, and discuss the fate of trace metals.

2. Methods

2.1. Reagents and materials

Ultra-high purity HCl, HF, HNO_3, HOAc, NH_3 (TAMAPURE-AA-10 and 100, Tama Chemicals) were used for cleaning of materials, sample preservation and preconcentration. Standard solutions of elements were prepared from commercially available standard solutions (NACALAI TESQUE). All solutions were stored in low-density polyethylene (LDPE, Nalge Nunc International) bottles, which were cleaned according to the methods of Kinugasa et al. (2005). Polycarbonate nucleopore filters (0.2 μm pore size, 47 mm diameter; Nuclepore, Costar) were cleaned according to methods described in Nakatsuka et al. (2007) and stored in MQW (Milli-Q Gradient-A-10 system, Millipore). A closed filtration system was constructed with PFA materials and LDPE bottles. The interior of the filtration system was cleaned successively with 6 M HF (TAMAPURE-AA-100), 0.1 M HCl (TAMAPURE-AA-10) and MQW. The cleaning of materials and preparation of solutions were carried out in a clean laminar flow hood while wearing polyethylene gloves.

2.2. Fe enrichment and patch observation during SEEDS II

The observation during SEEDS II was performed using the R/V *Hakuho Maru* (HK) and R/V *Kilo Moana* (KM) from 13 July to 27 August 2004. The Fe enrichment and observation during the first 2 weeks (days 0–12) and the last 4 days (days 23–26) were carried out using HK. The observation between days 13 and 22 was conducted using KM. The experimental site was located at 48.5°N, 165°E in the northwest subarctic gyre. Prior to the Fe enrichment, a preliminary survey of surface water confirmed that the area was HNLC ($NO_3^- > 18\,\mu M$ and chlorophyll-$a < 1\,\mu g\,L^{-1}$) and that the dissolved Fe concentration was low (~0.02 nM; Nishioka et al., 2009).

$FeSO_4 \cdot 7H_2O$ (1860 kg) and sulfur hexafluoride (SF_6) were dissolved in seawater on board and injected into surface water in an area of 64 km^2 on 20 July (days 0–1). Since the enriched Fe was rapidly lost from the patch until day 2 (<0.5 nM for total dissolved concentration), the second Fe enrichment ($FeSO_4 \cdot 7H_2O$, 950 kg) was executed in an area of 168 km^2 inside the patch between days 5–6. SF_6 was available to trace the Fe patch for the first 12 days. Since pCO_2 in the patch decreased significantly, it was used to trace the patch between days 13 and 26. General methods and results of SEEDS II were detailed in Tsuda et al. (2007) and references therein. Nishioka et al. (2009) have described the method of Fe enrichment and the distribution of Fe during SEEDS II.

2.3. Seawater sampling

Discrete seawater samples were collected from upper 150 m depths with two types of clean sampling devices during the HK cruise. Twelve liters of Niskin-X samplers attached to an epoxy-coated aluminum frame of a CTD-carousel system (Sea Bird Electronics) were used inside the patch. 10 L Niskin-X samplers were attached to a Kevlar hydro-wire and tripped with Teflon messengers outside the patch. The drain cock of the sampler was replaced with a Teflon one. The interior of the sampler was coated with Teflon and cleaned with detergent and HCl.

Seawater samples were subdivided into LDPE bottles. Immediately after collection, seawater (500 mL) was filtered through a Nuclepore filter using the closed filtration system in a shipboard Class 1000 clean room. The filtrate was acidified to pH 2.2 with 20% w/w HCl (TAMAPURE AA-10, 190 μL/100 mL of the filtrate) and stored until the determination of dissolved trace metals on land. The filter and particulate matter were taken in an acid-cleaned Petri dish and frozen until analysis on land.

During the KM cruise, seawater sampling was preformed by using Teflon coated Niskin-X samplers and Teflon messengers deployed on Kevlar hydro-wire. Filtration was carried out with an acid-cleaned 0.22-μm Durapore membrane filter (Cartridge type-Millipak 100, Millipore) in a clean hood on the deck. The filtrate was acidified to pH 2.2 with HCl as done during the HK cruise. No particulate sample was collected during the KM cruise.

2.4. Bottle incubation with Fe addition

Seawater for the bottle incubation experiment was collected using three Niskin bottles from 10 m depth outside the patch (47°N, 165°E) on day 24. The seawater was characterized by ~0.3 $\mu g\,L^{-1}$ of chlorophyll-a, >15 μM of NO_3^- and <0.1 nM of dissolved Fe. The seawater was homogenized in an acid-cleaned 25-L polycarbonate tank and filtered through a 202-μm mesh in order to remove mesozooplankton. The seawater was divided into 10-L fractions. One fraction was added with $FeCl_3$ stock solution to achieve a final Fe concentration of 1 nM (+Fe) and subdivided into 10 polycarbonate bottles (1 L). The other fraction was used as control seawater. This fraction was also subdivided into 10 other bottles. The cap of each bottle was sealed with parafilm and nylon tape. Each bottle was covered with a polyethylene bag and a shade cloth that reduced the light irradiance to ~35% of an ambient

value. Each of the nine +Fe and control bottles was incubated in a seawater tank on the deck, where the temperature was maintained at 12 °C using a circulator. The incubation proceeded for 10 days. The incubation time on day i is referred to T_i hereafter. The remnant +Fe and control bottles served as T_0 samples. Two +Fe and two control bottles were taken from the incubator on every T_i ($i = 2, 4, 6, 8$) for analysis. One +Fe and one control bottle were used as T_{10} samples.

Sampling was performed from each bottle to determine concentrations of dissolved and particulate trace metals, chlorophyll-*a* and nutrients ($Si(OH)_4$, NO_3^-+NO_2^- and PO_4^{3-}). Five hundred milliliters of seawater were filtered and acidified to determine the dissolved Co, Ni, Cu, Zn, Cd and Pb. The filter served as a sample for particulate Co, Ni, Cu, Zn, Cd and Pb. One hundred and fifteen milliliters of seawater were passed through a Whatman GF/F filter and chlorophyll-*a* on the filter was extracted into 6 mL of *N*,*N*-dimethylformamide (DMF) at −20 °C for 24 h (Suzuki and Ishimaru, 1990). The concentration was measured on board using a Turner Designs fluorometer. Ten milliliters of seawater for the determination of nutrients were placed in an acrylic tube and frozen until analysis on land. Eukaryotic phytoplankton was examined using a microscope to count the cell number and to identify the species composition at T_0 and T_{10}. Growth rates for the entire phytoplankton community ($\mu\,day^{-1}$) were calculated according to the following equation:

$$\mu = (\ln X_{10} - \ln X_0)/(T_{10} - T_0) \quad (1)$$

where X_{10} and X_0 are the total cell numbers for phytoplankton community at T_{10} and T_0, respectively.

2.5. Determination of dissolved and particulate trace metals

Dissolved trace metals were determined according to the previous method (Kinugasa et al., 2005). A 140-mL aliquot of seawater was adjusted to pH 5.0 ± 0.1 with 15 M AcOH–$AcONH_4$ (340 μL/100 mL of the sample solution) and dissolved trace metals were concentrated using a MAF-8HQ chelating adsorbent column at a flow rate of 2.1 mL min^{-1}. After rinsing with 40 mL of 0.05 M AcOH–$AcONH_4$, the metals were eluted with 0.8 M HNO_3 in the reverse direction of sample loading. Co, Ni, Cu, Zn, Cd and Pb in the eluate were measured with an inductively coupled plasma mass spectrometer (ICP-MS, ELAN DRC II, Perkin-Elmer) using isotopes of ^{59}Co, ^{60}Ni, ^{62}Ni, ^{63}Cu, ^{65}Cu, ^{66}Zn, ^{68}Zn, ^{111}Cd, ^{114}Cd, ^{206}Pb and ^{208}Pb. Concentrations of the analytes were calculated using a standard addition method. The standard added samples were measured just after the original sample. Since polyatomic ions of CaO^+ and MoO^+ interfere with the determination of Co and Cd, respectively, the interferences were corrected by the following formula:

$$\text{Co or Cd concentration} = (M_{\text{eluate}} - K \times I_{\text{eluate}})/S \quad (2)$$

where M_{eluate} is the intensity observed at m/z (mass/charge) = 59, 111 or 114 for the eluate, K is the intensity ratio of CaO/Ca or MoO/Mo observed for Ca or Mo standard solution, I_{eluate} is the intensity of Ca or Mo for the eluate, and S is the slope of the calibration line for the isotope of the analytes. Ca and Mo standard solutions were measured at appropriate intervals to correct changes in the CaO/Ca or MoO/Mo ratio.

Particulate trace metals were analyzed according to a previous method (Nakatsuka et al., 2007). The filter and particulate matter were placed in a 7 mL PFA decomposition vessels (DV-7, Sanai-Kagaku) and hydrolyzed in 750 μL of 20% (w/w) NH_3 with a microwave oven at 200 W for 5 min. The vessel was then mounted on a trace metal-clean evaporation system. The sample was evaporated to dryness at 210 °C for 20 min. The residue was added with 300 μL of 68% (w/w) HNO_3, 300 μL of 38% (w/w) HF and 300 μL of 68% (w/w) $HClO_4$, and digested using the microwave oven and evaporation system. After evaporation of the acids, the residues were dissolved in 1 mL of 0.8 M HNO_3. The sample pH was adjusted to 5.0 by adding buffer solution and the trace metals were determined by online column concentration–ICP-MS as follows: the sample was loaded on a MAF-8HQ column for 180 s (2.1 mL min^{-1}). After rinsing with 0.05 M AcOH–$AcONH_4$ for 180 s (2.1 mL min^{-1}), metals were eluted with 0.8 M HNO_3 (1.8 mL min^{-1}) in the reverse direction of sample loading. The eluate was directly introduced to ICP-MS, and ^{59}Co, ^{60}Ni, ^{62}Ni, ^{63}Cu, ^{65}Cu, ^{66}Zn, ^{68}Zn, ^{111}Cd, ^{114}Cd, ^{206}Pb and ^{208}Pb were concurrently measured. Calibration lines were obtained using standard solutions containing 0.05 M AcOH–$AcONH_4$. The concentrations were calculated from peak areas for each isotope.

Procedural blanks for the dissolved trace metals, which include acidification, buffering, concentration and determination were examined by using 140 mL of MQW as a sample. Procedural blanks for particulate trace metals were obtained using an acid-cleaned nucleopore filter. The detection limits were calculated as three times the standard deviation of the blanks. The blanks and detection limits are summarized in Table 1. The blanks for dissolved species were less than 5% of the concentrations of the dissolved trace metals in samples. The accuracy of our methods for dissolved and particulate Co, Ni, Cu, Zn, Cd and Pb was confirmed by the analysis of reference materials for seawater (NASS-5; National Research Council Canada) and algae (NIES CRM No. 3 chlorella, National Institute for Environmental Studies). Table 2 shows the analytical results of the reference materials. Our values agreed well with the certified values.

3. Results

All data on the dissolved and particulate trace metals during the mesoscale Fe enrichment are listed in Appendix. The data with parentheses are anomalous values on the vertical profiles and ignored in subsequent processing and discussion. Data on nutrients were taken from Saito et al. (2009), where details of the nutrient dynamics were described.

3.1. Distributions of trace metals before the mesoscale Fe enrichment

Vertical distributions of sigma-*t*, chlorophyll-*a* before the Fe enrichment (day 0) are shown in Fig. 1. Sigma-*t* was constant from surface to 20 m depth and increased downward, indicating a height of 20 m for the surface mixed layer. Chlorophyll-*a* was enriched at depths of 0–30 m (0.8–1.1 μg L^{-1}), below which the concentration decreased with depth.

Fig. 2 shows the vertical distributions of dissolved and particulate Co, Ni, Cu, Zn, Cd and Pb on day 0. Dissolved Ni, Zn and Cd exhibited low concentrations in the surface mixed layer and gradually increased with depth, which were similar to nutrients. The concentrations ranged between 5.0 and 6.3 nM for Ni, 1.4–8.7 nM for Zn and 0.46–0.99 nM for Cd in the upper water column between 0 and 150 m. On the other hand, particulate Ni, Zn and Cd were enriched at depths less than 40 m with the concentrations ranging between 0.039 and 0.068 nM for Ni, 0.28–0.53 nM for Zn, 0.017–0.045 nM for Cd, and decreased with depth below 40 m. Dissolved Co varied between 56 and 75 pM throughout the upper water column. Particulate Co had two maxima of 2.4 pM at surface and 1.6 pM at 40–50 m. Dissolved Cu concentration scattered in the upper water column (1.7–2.6 nM). Particulate Cu had a clear maximum (0.19 nM) at the surface, although the concentration was nearly constant (0.04 ± 0.01 nM) below 10 m. Dissolved Pb varied

Table 1
Summary of procedural blank and detection limit for dissolved and particulate trace metals.

Elements	Units	Dissolved species			Particulate species		
		n	Procedure blank	Detection blank	*n*	Procedure blank	Detection limit
Co	pM	5	0.1±0.1	0.4	12	0.9±0.1	0.3
Ni	nM	5	0.01±0.01	0.02	12	0.170±0.005	0.015
Cu	nM	5	0.010±0.005	0.01	12	0.005±0.001	0.002
Zn	nM	5	0.02±0.02	0.06	12	0.05±0.02	0.06
Cd	nM	5	0.0007±0.0004	0.001	12	0.0003±0.0002	0.001
Pb	pM	5	0.5±0.2	0.7	12	4.6±0.3	0.9

Table 2
Analytical results of trace metals in reference materials for seawater (NASS-5) and algae (NIES CRM no. 3).

Element	NASS-5			NIES CRM no. 3		
	Certified value (nM)	This study		Certified value (mg kg^{-1})	This study	
		n	(nM)		*n*	(mg kg^{-1})
Co	0.186±0.05	3	0.188±0.004	0.870±0.05	12	0.833±0.05
Ni	4.08±0.45	3	4.03±0.15		12	
Cu	4.57±0.71	3	4.41±0.05	3.5±0.3	12	3.5±0.3
Zn	1.55±0.59	3	1.34±0.12	20.5±1.0	12	19.8±1.4
Cd	0.21±0.03	3	0.19±0.01	0.026[a]	12	0.027±0.004
Pb	0.039±0.02	3	0.035±0.001	0.6[a]	12	0.6±0.1

[a] Information value.

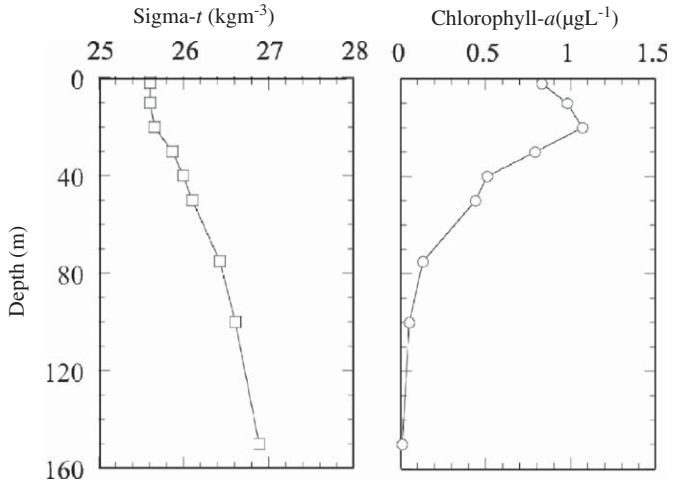

Fig. 1. Vertical distributions of sigma-*t* and chlorophyll-*a* before the Fe enrichment (day 0).

between 50 and 60 pM in the upper water column. Particulate Pb decreased from 6.2 pM at surface to 4.0 pM at 50 m.

The mean concentrations of dissolved Co, Ni, Cu, Zn, Cd and Pb in the surface mixed layer were 70±4 pM, 4.9±0.1, 2.1±0.4, 1.6±0.3, 0.48±0.01 nM and 52±2 pM, respectively. The mean concentrations of particulate species were 1.7±0.7 pM for Co, 0.052±0.015 nM for Ni, 0.09±0.08 nM for Cu, 0.46±0.06 nM for Zn, 0.037±0.001 nM for Cd and 5.7±0.5 pM for Pb (day 0 in Table 3).

3.2. Variations in chlorophyll-a, nutrients and trace metals in the surface mixed layer during the mesoscale Fe enrichment

Temporal changes in chlorophyll-*a* concentrations in the surface mixed layer are plotted in Fig. 3. Concentrations of chlorophyll-*a* inside the patch nearly tripled by days 10–13 and then gradually decreased. Tsuda et al. (2007) reported that the bloom was dominated by non-diatom phytoplankton, while oceanic diatoms of *Pseudo-nitzschia* spp. and *Neodenticula seminae* also increased during the bloom. According to the size-fractionated chlorophyll-*a* data, micro-, nano- and pico-sized chlorophyll-*a* accounted for 27%, 43% and 30% of the total chlorophyll-*a* before the increase in phytoplankton on days 0–2. The ratio did not change largely during the developing phase 1 (days 2–8, Fig. 3) and then the contribution of pico-phytoplankton increased during developing phase 2 (days 8–12, Fig. 3).

Temporal changes in concentrations of NO_3^-+NO_2^-, $Si(OH)_4$ and PO_4^{3-} in the surface mixed layer are plotted in Fig. 4. Concentrations of NO_3^-+NO_2^- and PO_4^{3-} inside the patch decreased by 3 and 0.1 μM in the developing phases, respectively. The concentrations continued to decrease after day 13 and showed minimums on day 21. The differences in the concentrations between inside and outside the patch on day 12 were 2 μM for NO_3^-+NO_2^- and 0.1 μM for PO_4^{3-}. Concentrations of $Si(OH)_4$ decreased with time, and no significant differences were observed between the inside and outside throughout the experiment.

Fig. 5 shows temporal changes in dissolved and particulate concentrations for Co, Ni, Cu, Zn, Cd and Pb in the surface mixed layer. There was no significant difference in the concentrations of dissolved Co, Ni, Cu, Zn and Pb between inside and outside the patch. Dissolved Co, Ni and Pb concentrations remained nearly constant over the course of the experiment. Concentrations of dissolved Cu decreased until days 18–21 and then returned to the initial level at the end of the experiment. Dissolved Zn showed a similar change with dissolved Cu, although the concentrations varied largely during the observation on KM. Dissolved Cd inside the patch was significantly higher than outside the patch (*t*-test, $p<0.05$) on day 2. The concentration inside the patch slightly decreased from 0.48±0.01 nM on day 2 to 0.46±0.01 nM on day 12, and rapidly decreased to 0.35±0.01 nM on days 16–17. In contrast, dissolved Cd concentrations outside the patch remained constant (0.35±0.03 nM) over the course of the experiment.

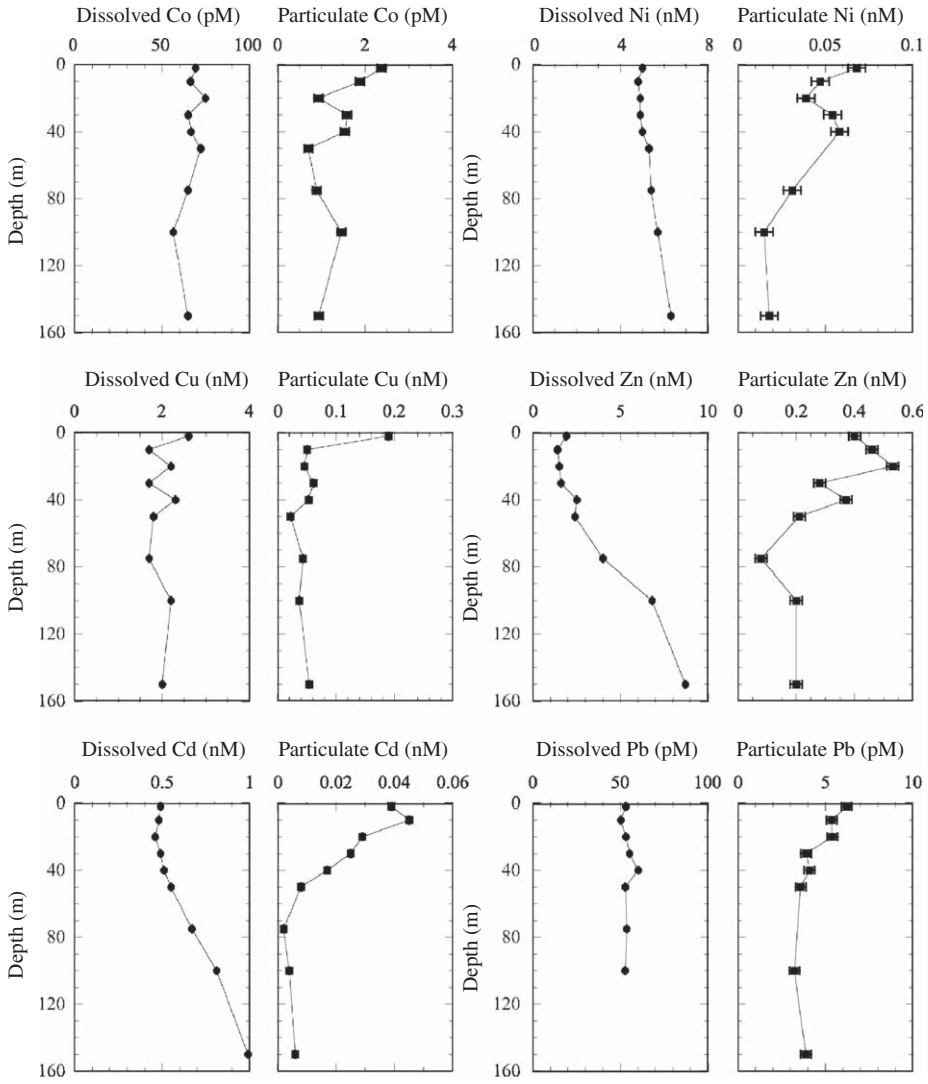

Fig. 2. Vertical distributions of dissolved and particulate Co, Ni, Cu, Zn, Cd and Pb on day 0. Filled circles and the solid line indicate the dissolved species ($<0.2\,\mu m$). Filled squares and the solid line indicate the particulate species ($>0.2\,\mu m$). The error bars represent 2σ of procedural blanks.

Table 3
Summary of particulate trace metal concentrations before and after the Fe enrichment.

Element	Unit	Before the Fe enrichment[a]	After the Fe enrichment			
			Inside the patch[b]		Outside the patch[c]	
		Day 0	Mean ± sigma	Variation	Mean ± sigma	Variation
Co	pM	1.7 ± 0.7	2.4 ± 0.6	1.3–3.8	2.9 ± 0.9	1.7–3.7
Ni	nM	0.052 ± 0.015	0.067 ± 0.019	0.043–0.82	0.069 ± 0.012	0.052–0.081
Cu	nM	0.09 ± 0.08	0.12 ± 0.04	0.06–0.16	0.09 ± 0.03	0.06–0.11
Zn	mM	0.46 ± 0.06	0.45 ± 0.09	0.36–034	031 ± 0.11	0.39–0.64
Cd	nM	0.037 ± 0.001	0.047 ± 0.010	0.037–0.057	0.052 ± 0.007	0.037–0.056
Pb	pM	5.7 ± 0.5	43 ± 1.1	2.9–6.1	5.2 ± 0.7	4.5–6.5

[a] Average concentrations in the surface mixed layer on day 0. Uncertainty represents the standard deviation of the concentrations in the upper 20 m.
[b] Average concentrations in the surface mixed layer inside the patch between days 2 and 12. Uncertainty represents the standard deviation of all data observed for the upper 20 m depths. Variation indicates concentration ranges of variations between days 2 and 12.
[c] Average concentration in the surface mixed layer outside the patch between day 2 and 12. Uncertainty represents the standard deviation of all data observed for the upper 20 m depths. Variation indicates concentration ranges of variations between days 2 and 11.

Average concentrations for dissolved species inside the patch were 67 ± 3 pM for Co, 4.9 ± 0.1 nM for Ni, 2.0 ± 0.3 nM for Cu, 1.5 ± 0.4 nM for Zn, 0.42 ± 0.05 nM for Cd and 55 ± 2 pM for Pb throughout the experiment (days 0–26).

Data on particulate trace metals in the developing phases (days 2–12) are summarized in Table 3. The mean concentrations of particulate trace metals inside the patch varied between 1.3–3.8 pM for Co, 0.043–0.082 nM for Ni, 0.06–0.16 nM for

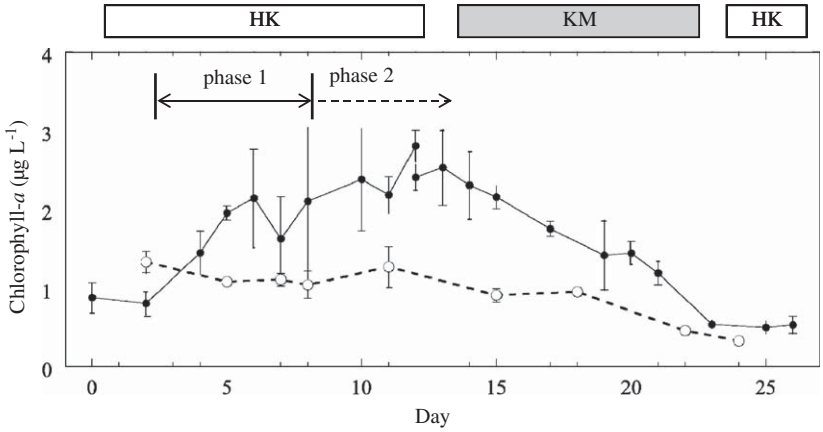

Fig. 3. Temporal changes in chlorophyll-*a* concentrations in the surface mixed layer (<20 m). Filled circles and the solid line indicate mean concentrations inside the patch. Open circles and broken line indicate mean concentrations outside the patch. The error bars represent 2σ of the concentration in the surface mixed layer. Phase 1 represents the period when all of the micro-, nano- and pico-sized chlorophyll-*a* increased (days 2–8). Phase 2 represents the periods when pico-phytoplankton increased (after day 8). KH and KM represent the observation period using R/V *Hakuho Maru* and R/V *Kilo Moana*, respectively.

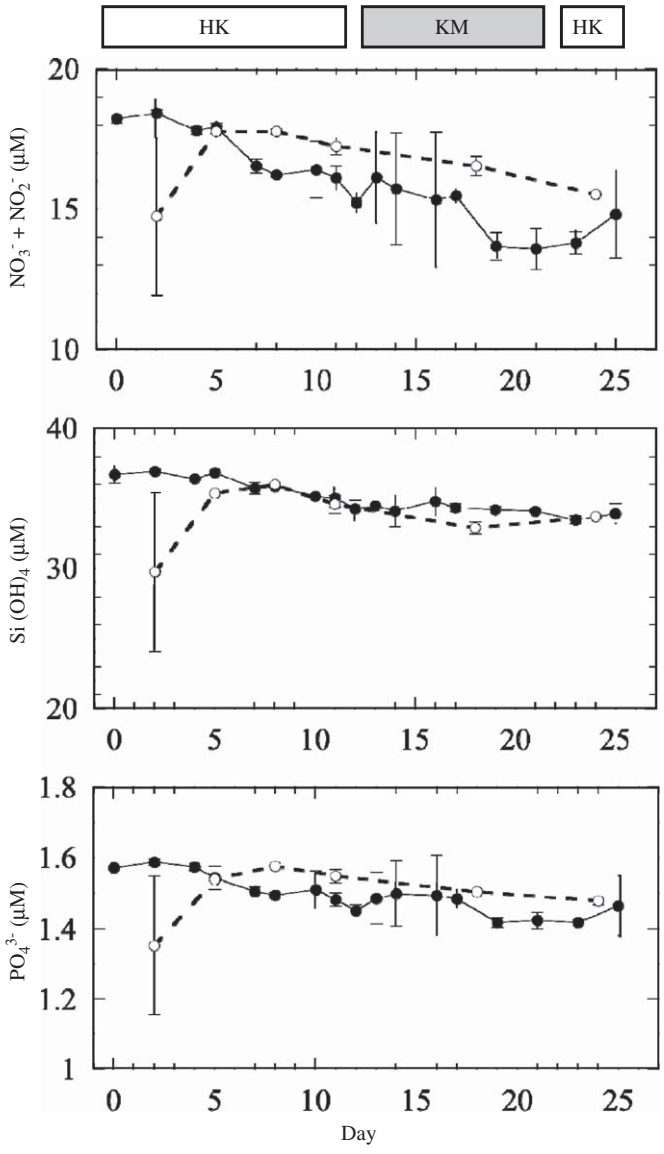

Fig. 4. Temporal changes in concentrations of NO_3^-+NO_2^-, $Si(OH)_4$ and PO_4^{3-} in the surface mixed layer (<20 m). Filled circles and the solid line indicate mean concentrations inside the patch. Open circles and the broken line indicate mean concentrations outside the patch. Error bars represent 2σ of the concentration in the surface mixed layer.

Cu, 0.36–0.54 nM for Zn, 0.037–0.057 nM for Cd and 2.9–6.1 pM for Pb on days 2–12. Particulate Co, Ni and Cd inside the patch showed maximums on days 7–8 and then returned to the initial levels. The days of the maximums coincided with the transition between phase 1 and 2 (Fig. 3). Particulate Cu inside the patch had two maximums on days 5 and 8 and showed a higher value on day 23. Concentrations of particulate Zn and Pb inside the patch slightly decreased over the course of t he experiment. Outside the patch, particulate trace metals except Cu were relatively constant until day 12 and slightly decreased until day 24. There were no statistically significant differences in the concentrations between inside and outside the patch.

3.3. Bottle incubation with Fe addition

Temporal changes in chlorophyll-*a*, $Si(OH)_4$, NO_3^-+NO_2^- and PO_4^{3-} in the shipboard incubation are given in Fig. 6. A large increase in chlorophyll-*a* was observed in the +Fe bottles (8.9 μg L^{-1} at T_{10}), while the control bottles showed a slight increase (1.5 μg L^{-1} at T_{10}). Nutrients consumed in the +Fe bottles were 6.8 μM for NO_3^-+NO_2^- and 0.36 μM for PO_4^{3-} over 10 days, while those in the control bottles were 2.0 μM for NO_3^-+NO_2^- and 0.13 μM for PO_4^{3-}. The decrease in $Si(OH)_4$ differed a little between the +Fe (4.2 μM) and the control (3.9 μM) bottles.

Phytoplankton biomass was dominated by eukaryotes. Species compositions of eukaryotic phytoplankton are shown in Table 4. Autotrophic nanoplankton (517 cells mL^{-1}), oceanic diatoms of *Fragilariopsis* sp. (103 cells mL^{-1}) and *Pseudo-nitzschia* sp. (252 cells mL^{-1}) were dominant in the +Fe bottle at T_{10}. Although the species composition in the control bottle was similar to that in the +Fe bottle, the cell numbers at T_{10} were nearly one-third of those in the +Fe bottle. The growth rates of the entire phytoplankton community were calculated to be 0.29 and 0.17 day^{-1} for +Fe and the control, respectively.

Temporal changes in the trace metals are shown in Fig. 7. All the dissolved metals except Ni and Cu decreased in the +Fe bottles with the greatest changes observed for Zn and Cd. Dissolved Zn and Cd in the control bottles also decreased, but the decreases were smaller than those in the +Fe bottles. Particulate trace metals in the +Fe bottles increased in association with chlorophyll-*a*, becoming significantly higher than those in the control bottles. Particulate Co, Ni, Cu and Pb showed a 2–3 fold increase, and the particulate fraction at T_{10} accounted for 15%, 3%,

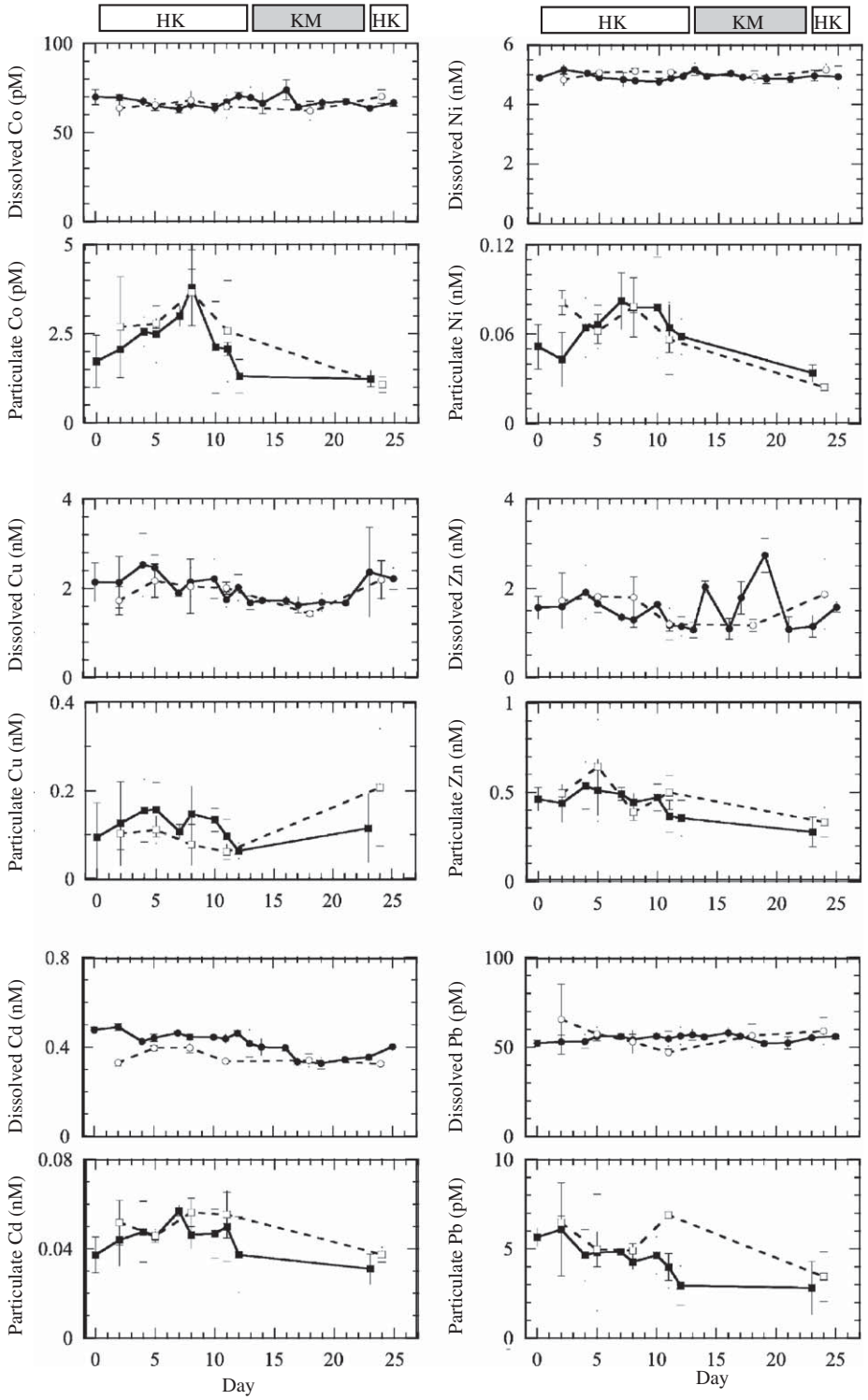

Fig. 5. Temporal changes in dissolved and particulate concentrations for Co, Ni, Cu, Zn, Cd and Pb in the surface mixed layer. Filled circles and squares with a solid line indicate mean values for dissolved (<0.2 μm) and particulate (>0.2 μm) species inside the patch, respectively. Open circles and squares with a broken line indicate the mean values for dissolved and particulate species outside the patch, respectively. Error bars represent 2σ of the concentration in the surface mixed layer.

13% and 21% of the total concentrations (sum of dissolved and particulate trace metal concentrations), respectively. Particulate Zn and Cd measured at T_{10} in the +Fe bottle were 0.58 and 0.18 nM, which accounted for 43% and 45% of the total concentrations, respectively. Particulate Zn and Cd in the control bottle were 0.42 and 0.12 nM at T_{10}, which accounted for 32% and 28% of the total concentrations, respectively.

4. Discussion

4.1. Dissolved and particulate trace metals before the mesoscale Fe enrichment

There are some reported data on dissolved Co, Ni, Cu, Zn, Cd and Pb in the vicinity of the study area (Table 5). Fujishima et al.

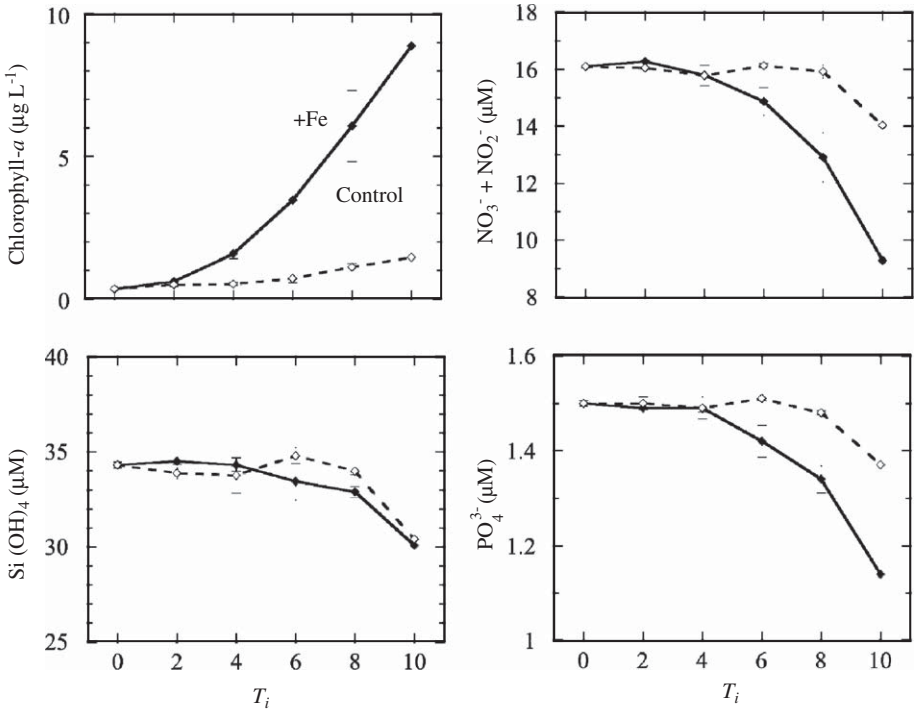

Fig. 6. Temporal changes in chlorophyll-*a*, $Si(OH)_4$, NO_3^-+NO_2^- and PO_4^{3-} in the bottle incubation. Filled diamonds and the solid line indicate the +Fe bottle. Open diamonds and the broken line indicate the control bottle. The error bars for T_0 and T_{10} represent 2σ of the procedural blanks. Error bars for T_{2-8} represent 2σ of the concentrations observed for the replicate bottles.

Table 4
Species composition of phytoplankton (*eukaryotes*) in the incubation bottles (cells mL^{-1}).

Phytoplankton species	Control bottle		+Fe bottle	
	T_0	T_{10}	T_0	T_{10}
Diatoms				
Centric diatoms				
Thalassiosira sp.		1		5
Thalassiosiraceae	4	5		2
Chaetoceros convolutes		1		
Pennate diatoms		2		2
Thalassiothrix longissima		1		1
Naviculaceae cylindrotheca		1		5
Closterium	4	54	1	103
Fragilariopsis sp.		3		1
Neodenticula seminae	1	71	1	252
Pseudo-nitzschia sp.				
Dinoflagellates				
Prorocentrum balticum		1	1	1
Gimnodiniales	3	16	4	15
Peridiniales	1			1
Other eukaryotes				
Autotrophic nanoplankton	32	86	11	517
Cryptophyceae	6	3	16	10
Prymnesiophyceae-Haptophyceae	7	22	14	43
Prymnesiophyceae				
Phaeocystis sp.				
Coccolothophorids	2	27	2	34
Haptophyceae				
Coccolithophorids				

(2001) reported dissolved Co of 30–51 pM, Ni of 4.8–5.3 nM and Zn of <0.4–1.5 nM at 44°05′N, 161°44′E (0–148 m depths). Dissolved Cd ranged between 0.37 and 0.93 nM at depths of 0 and 149 m, 44°00′N, 155°00′E (Abe, 2002). Kinugasa et al. (2005) addressed the dissolved trace metals in the upper water column (0–75 m) before SEEDS I, where dissolved Co, Ni, Cu, Zn and Cd ranged between 32 and 36 pM, 5.00–5.33, 1.59–1.88, 2.2–4.6 and 0.37–0.56 nM, respectively. More recently, total dissolved Cu was measured to be 2.2 nM in surface water at 46°6′N, 170°2′E (Moffett and Dupont, 2007). There are no reported data on dissolved Pb. Our results are in accord with these data except Co. The sampling season and area were the same between Kinugasa et al. (2005) and our study. However, there is a discrepancy in dissolved Co concentrations. This may reflect temporal variation, because Co is more readily scavenged than the other metals.

There are no available data on the particulate trace metals in this region, while several studies have described the total concentrations of trace metals in unfiltered seawater. Kinugasa et al. (2005) analyzed acid dissolvable species in the seawater samples, which were unfiltered, acidified to pH 2.2 with HCl and stored for 20 months at an ambient temperature before analysis. According to their data, the acid-dissolvable concentrations in the upper water column were 5.17–5.63 nM for Ni, 1.76–2.39 nM for Cu, 3.15–4.92 nM for Zn and 0.50–0.67 nM for Cd. The total Cd concentration was 0.49–0.82 nM at depths of 30–123 m at 51°28′N, 165°2′E (Lacan et al., 2006). In our study, it is assumed that the sum of dissolved and particulate trace metal concentration represents the total concentration. Total Ni, Cu, Zn and Cd are 4.6–6.3, 1.7–2.7, 1.8–8.9 and 0.49–0.99 nM, respectively. These concentrations are in good agreement with the literature data except for Co.

Our data indicate the predominance of dissolved Co (>97%), Ni (>99%), Cu (>93%), Zn (>74%), Cd (>91%) and Pb (>90%) in the western North Pacific. The results are similar to those of Zn and Cd observed in the central North Pacific Ocean (Bruland et al., 1994) and those of Ni, Cu, Zn and Cd in the Southern Oceans (Frew et al., 2001). The relationships between dissolved trace metals (Ni, Zn and Cd) and PO_4^{3-}, and between particulate trace metals (Ni, Zn and Cd) and chlorophyll-*a* throughout the upper water column are shown in Fig. 8. Dissolved Ni, Zn and Cd on day 0 were lineally correlated with PO_4^{3-}, with a correlation coefficient (r) being

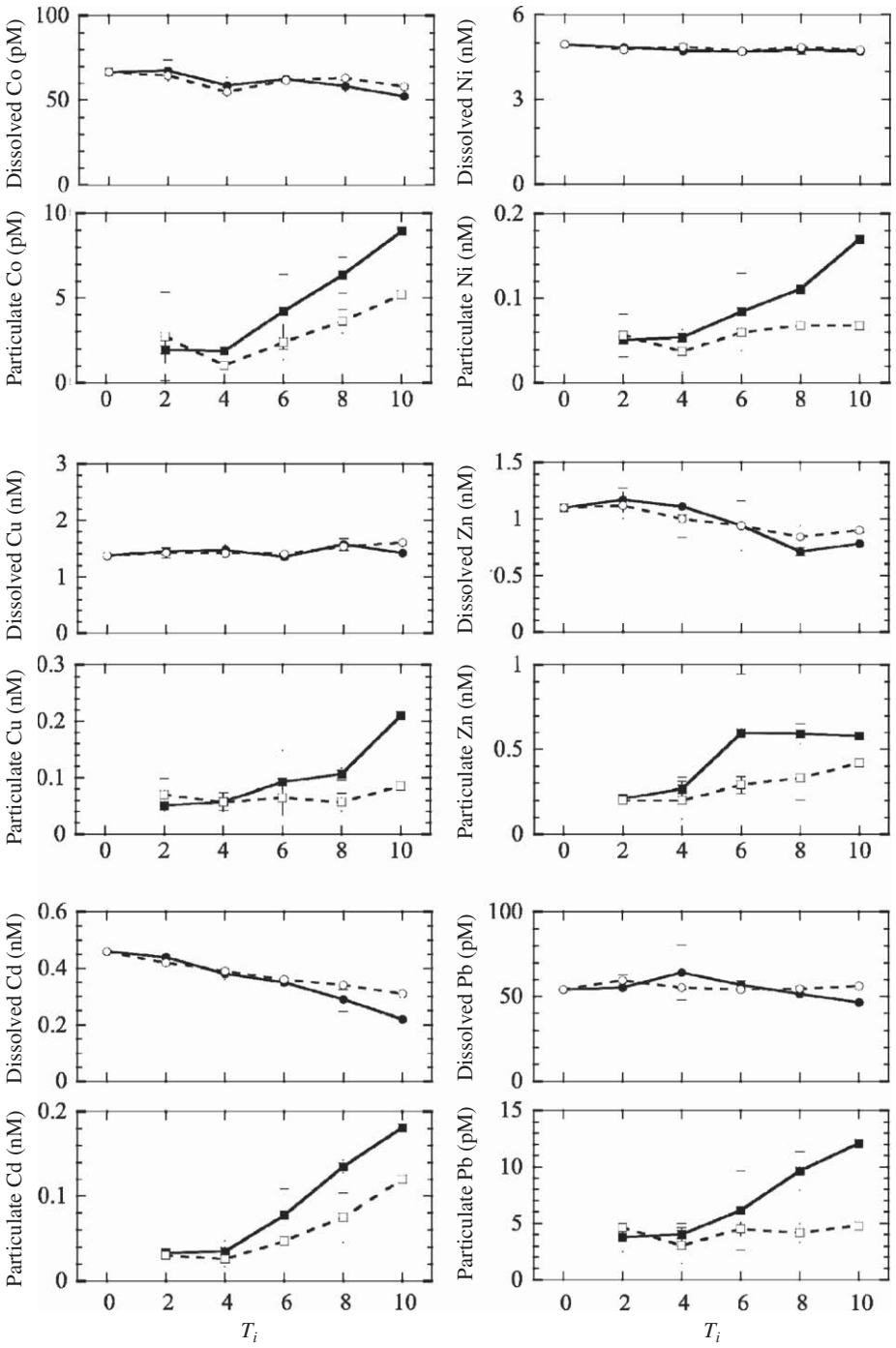

Fig. 7. Temporal changes in the trace metals in the bottle incubation. Filled circles and squares with a solid line indicate dissolved (<0.2 μm) and particulate (>0.2 μm) species in the +Fe bottles, respectively. Open circles and squares with a broken line indicate dissolved and particulate species in the control bottles. Error bars for T_{10} represent 2σ of the procedural blanks. Error bars for T_{2-8} represent 2σ of the concentrations observed for the replicate bottles.

higher than 0.98. Moreover, particulate Ni, Zn and Cd exhibited a positive correlation with chlorophyll-*a* ($r = 0.71$–0.91). These correlations indicate that biogeochemical cycling mainly controls the distributions of Ni, Zn and Cd in the study area.

4.2. *Differences in biological responses between the bottle incubation and the mesoscale Fe enrichment*

The shipboard incubation experiment revealed that addition of 1 nM Fe caused a large increase in chlorophyll-*a* and drawdown of nutrients for 10 days (Fig. 5). These results indicate that Fe deficiency was a limiting factor for the phytoplankton growth. However, the increase in chlorophyll-*a* observed during the mesoscale Fe enrichment was limited to $\sim 2\,\mu g\,L^{-1}$ (Fig. 3). It must be considered whether there was a difference in Fe concentration between the bottle incubation and the mesoscale Fe enrichment. Added Fe would have been subject to export and dilution losses in the mesoscale Fe enrichment, whereas they do not occur in bottle incubation. Nishioka et al. (2009) investigated dissolved and total dissolved Fe concentrations during the mesoscale Fe enrichment. They observed 1.73 nM of total

Table 5
Comparison of dissolved and total Co. Ni, Cu Zn, Cd and Pb concentration in the western North Pacific.

Element	Unit	Dissolved concentration					Total concentration			
		SEEDS II[a]	SEEDS I[b]	46°6′N 170°2′E[c]	44°0′N 155°0′E[d]	44°1′N 161°0′E[e]	SEEDS II[a]	SEEDS I[b]	45°1′N 165°2′E[f]	51°3′N 165°2′E[g]
		0–150 m	0–75 m	Surface	0–149 m	0–148 m	0–150 m	0–75 m	0–99 m	30–123 m
Co	pM	56–75	32–36			30–51	58–76	26–36		
Ni	nM	4.8–6.3	5.00–5.33			4.8–5.3	4.9–63	5.17–5.63	2.4–5.1	
Cu	nM	1.7–2.6	1.59–1.88	2.2			1.7–2.7	1.76–239	0.9–2.0	
Zn	nM	1.4–8.7	2.2–4.6			<0.4–13	1.8–8.9	3.2–4.9		
Cd	nM	0.46–0.99	0.37–0.56		0.37–0.93		0.49–0.99	0.50–0.67		0.49–0.82
Pb	pM	53–60					56–64			

[a] This study. Dissolved trace metals were concentrated by MAF-SHQ chelating adsorbent. Paniculate trace metals were determined by using on-line column preconcentration–ICP-MS alter acid digestion.
[b] Data from Kinugasa et al. (2005). Dissolved trace metals were concentrated by MAF-8HQ chelating adsorbent. Acid-dissolvable species in the unfillered seawater samples was acidified to pH 22 with IICI and stored for 20 months at an ambient temperature before column extraction.
[c] Data from Moffett and Dupont (2007). Co speciation was characterized by using cathodic stripping voltammetry with the competing ligands benzoylaceton and salicylaldoxime.
[d] Data from Abe (2002). Dissolved Cd in an unfillered sample was concentrated by the APDC (coprecipitation method).
[e] Data from Fujtshima et al. (2001). Dissolved trace metals were concentrated by MAF-8HQ chelating adsorbent. Acid dissolvable species in the unaltered seawater samples was acidified to pH 22 with HCl and stored at an ambient temperature before column extraction.
[f] Data from Noriki et al. (1998).
[g] Data from Lacan et al. (2006). Cd in the unfiltered seawater sample was concentrated by using chelex-100 chelating resin.

dissolved Fe and 1.38 nM of dissolved Fe at 5 m depth on day 1. The concentrations of Fe decreased to 0.92 nM for total dissolved and 0.14 nM for dissolved on day 11. Although the Fe concentrations in the patch decreased with time probably by export and dilution losses, they were comparable to those in the +Fe bottles at least during the developing phases. Thus, the export and dilution losses of Fe are not the primary reason underlying the reduced increase in chlorophyll-*a* during the mesoscale Fe enrichment relative to the incubation.

Grazing by mesozooplankton is a convincing explanation for the differences in phytoplankton biomass between the two experiments. We removed the mesozooplankton from the incubation bottles, which is likely to lead more favorable conditions for a preferential increase in phytoplankton (Banse, 1991). On the other hand, mesozooplankton biomass, which was dominated by copepods (*Neocalanus plumchrus*), increased exponentially from day 5 to day 21 in the mesoscale Fe enrichment (Tsuda et al., 2009). It was suggested that copepods grazed down Fe-induced diatom growth, resulting in the weak response of phytoplankton during the mesoscale Fe enrichment.

4.3. Dynamics of trace metals during the mesoscale Fe enrichment

Here, we considered mass balance of nutrients and trace metals in the surface mixed layer inside the patch between days 0 and 12 (Fig. 9). The decreases in dissolved nutrients were 2.5 μM for $Si(OH)_4$, 3.0 μM for NO_3^-+ NO_2^- and 0.1 μM for PO_4^{3-}. These data give a mole ratio of $Si_{25}N_{30}P_1$. The Si/P ratio is in the range for the bottle incubation (Table 6), while the N/P ratio is slightly high. These results suggest that the decreases in dissolved nutrients are mainly due to uptake by phytoplankton, and that the effect of convection and advection can be ignored. The decreased inventory of dissolved nutrients in the surface mixed layer was 50 mmol m^{-2} for Si, 60 mmol m^{-2} for N and 2 mmol m^{-2} for P. These nutrients should have been transformed into particulate matter. Settling particles were collected at 40 m depth inside the patch, and their nutrient contents were determined (Aramaki et al., 2009). The observed Si, N and P fluxes were 1.9–3.7, 3.0–4.3, 0.075–0.102 mmol m^{-2} day^{-1}, resulted in the integrated flux of 35, 41 and 1.0 mmol m^{-2} for 12 days, respectively. These values accounted for 68% for Si, 70% for N, 42% for P of the decrease in the inventory. It is likely that the rest of the produced particulate species remained in the surface mixed layer as particulate species.

Although the phytoplankton species composition of the mesoscale Fe enrichment slightly differed from that of the bottle incubation (Table 4), we assume that the elemental ratio of phytoplankton during the mesoscale Fe enrichment is equal to that for the +Fe bottles (Table 6). The uptake of trace metals by phytoplankton associated with the drawdown of 0.1 μM PO_4^{3-} would be 2 pM for Co, 0.03 nM for Ni, 0.05 nM for Cu, 0.10 nM for Zn and 0.042 nM for Cd. When 42% of the particulate trace metals have been lost as settling particles in company with nutrients, the increase in particulate species in the surface mixed layer will be 1.2 pM for Co, 0.02 nM for Ni, 0.03 nM for Cu, 0.06 nM for Zn and 0.024 nM for Cd. These values are comparable with the variations in particulate metals inside and outside the patch (Table 3). Thus, it is reasonable that significant changes in particulate Co, Ni, Cu and Zn were not observed in the mesoscale Fe enrichment.

Moreover, it is likely that Pb was scavenged by biogenic particles during the developing phases. Assuming that the Pb/P ratio was equal between the incubation and the mesoscale Fe enrichment, the increase in particulate Pb would be 2.4 pM in the surface mixed layer. In reality, the particulate Pb concentration gradually decreased from 5.7 ± 0.5 pM on day 0 to 2.9 ± 1.1 pM on day 12. It is inferred that particulate Pb was effectively removed and vertically exported out of the mixed layer. Although very little is known of the nature of scavenging, enhanced biomass and grazing of mesozooplankton may be one of the reasons for the effective export losses.

4.4. Effect of Fe addition on elemental stoichiometry in marine phytoplankton

The bottle incubation experiments indicate that Fe addition leads to an increase in phytoplankton biomass and to transformation of trace metals from dissolved to particulate species (Fig. 7). The increases in the concentrations of particulate trace metals between T_2 and T_{10} were compared with the drawdown of dissolved trace metals. The increase accounted for 45% for Co, 92% for Ni, 533% for Cu, 95% for Zn, 71% for Cd and 93% for Pb of

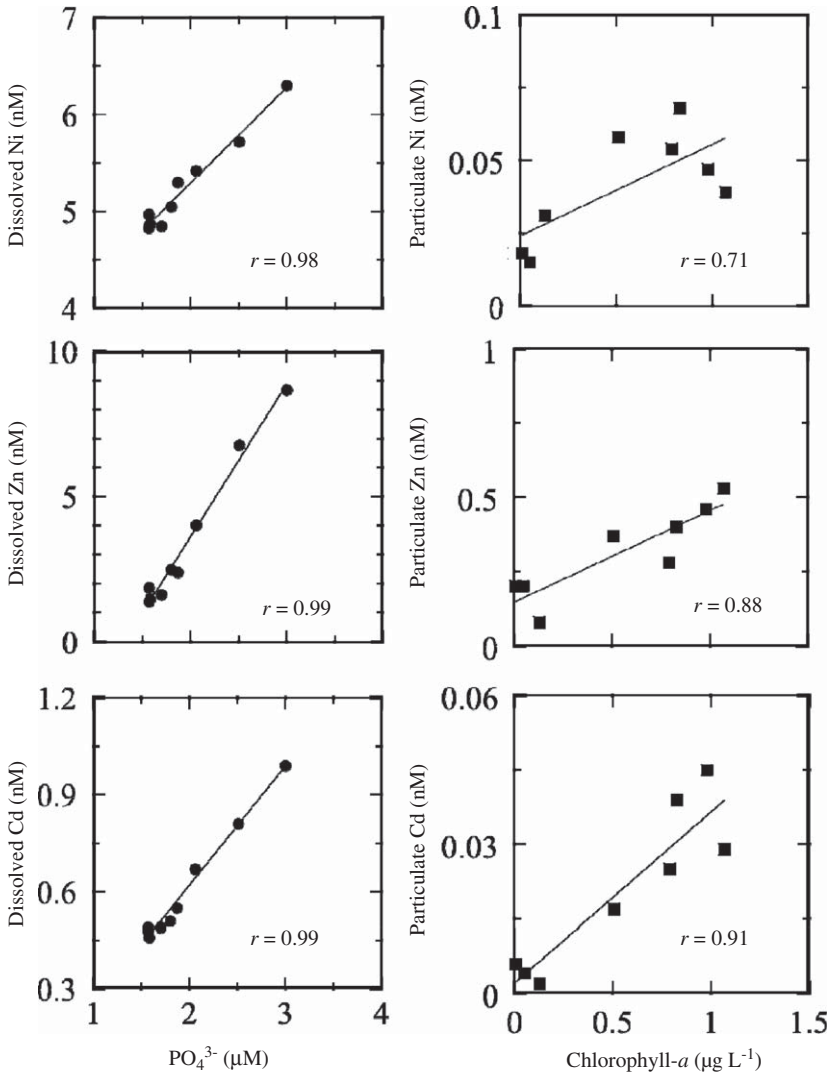

Fig. 8. Relationships between dissolved trace metals (Ni, Zn and Cd) and PO_4^{3-}, and between particulate trace metals (Ni, Zn and Cd) and chlorophyll-*a* are in the upper water column (<150 m) on day 0.

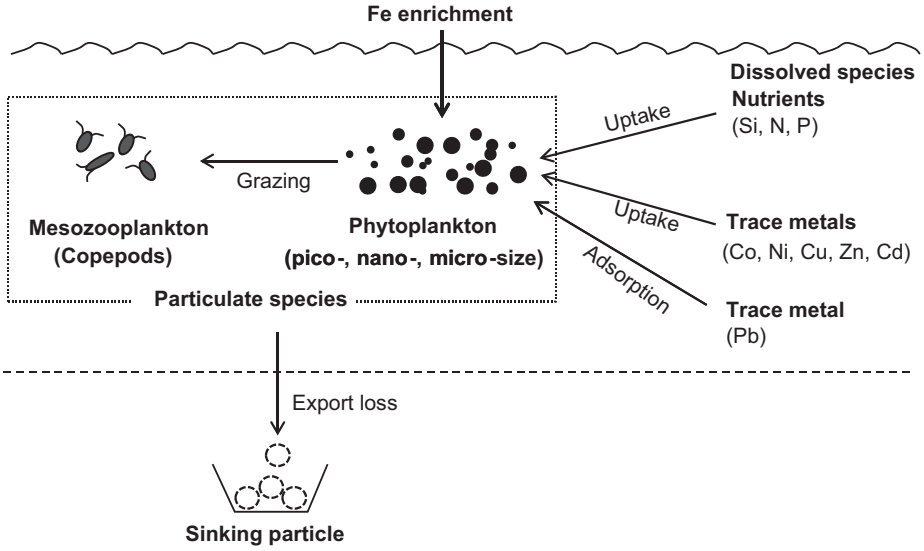

Fig. 9. A diagram showing behaviors of nutrients and trace metals inside the patch.

Table 6
Comparison of growth rate and elemental ratio normalized to *P*.

Study/treatment	Growth rate (day^{-1})	Element ration normalized to P						
		Nutrient/Pmol/mol		Metl/Pmmol/mol				
		Si	N	Co	Ni	Cu	Zn	Cd
This study/control[a]	0.17	26	15	0.019±0.020			1.7±0.2	0.66±0.03
This study/+Fe[b]	0.29	13	20	0.020±0.002	0.33±0.01	0.46±0.01	1.0±0.1	0.42±0.02
Ho et al. (2003)/Fe replete[c]			16	0.19 (0.13)		0.38 (0.35)	0.8 (0.52)	0.21 (0.22)
Kinugasa et al. (2005)/Fe patch[d]		27	16	0.023	0.61	0.38	1.2	0.054
Takeda (1998)/control[e]	0.14	31±7	12±0.5					
Takeda (1998)/+Fe[f]	0.49	14±6	12±3					
Cullen et al. (2003)/control[g]	0.15			0.29±0.01		0.51±0.01	3.96±0.09	0.62±0.01
Cullen et al. (2003)/+Fe[h]	0.28			0.10±0.004		0.60±0.01	2.91±0.09	0.44±0.01

[a] Si/P and N/P ratio was calculated from the drawdown of dissolved nutrients between and T_2 and T_{10} this study.
[b] Metal/P ratio was calculated from increases in particulate metals and drawdown of dissolved PO_4^{3-} between T_2 and T_{10}. SD represents the analytical uncertainty of the measurement (2σ).
[c] Data from Table 4 in Ho et al. (2003). Elemental quotas of marine phytoplankton (15 species) grown in Fe-repleted culture. Numbers in the parentheses represent one SD.
[d] Data from Table 3 in Kinugasa et al. (2005). Elemental ratio calculated from consumption ratio of dissolved species in the surface mixed layer during SEEDS I.
[e] Natural phytoplankton assemblages in the subarctic Pacific were grown in bottles without Fe addition.
[f] Natural phytoplankton assemblages in the subarctic Pacific were grown in bottles with Fe addition (1.1 nM).
[g] Natural phytoplankton assemblages in the Southern Ocean were grown in bottles without Fe.
[h] Natural phytoplankton assemblages in the Southern Ocean were grown in bottles with Fe addition (1 nM).

the drawdown in the +Fe bottle, and 38% for Co, 65% for Ni, 101% for Zn, 76% for Cd and 4% for Pb in the control bottle. These results suggest that most of the drawdown of dissolved species was incorporated into particulate matter. The disagreement for Cu and Pb may be attributed to a large error in the drawdown due to a high background, and that for Co may be attributed to adsorption onto the bottle wall. A potential explanation for the transformation is coprecipitation with Fe oxyhydroxide. However, the transformation was not significant in the mesoscale Fe patch, although the Fe concentration was comparable with that in the +Fe bottles. Thus, it is reasonable to ascribe the transformation to uptake by phytoplankton.

Here, we estimated the elemental stoichiometry in phytoplankton using the data on incubation. We present phosphorous normalized ratios, since they are often used by oceanographers and make comparison possible between plankton samples independent of cell volumes (Ho et al., 2003; Quigg et al., 2003). The elemental ratios (metal/P) were calculated from the drawdown of dissolved PO_4^{3-} and the increase in particulate metals between T_2 and T_{10} (Table 6). The average elemental ratio in the +Fe bottles is expressed by the following formula:

$$(Si_{13}N_{20}P_1)_{1000}Zn_{1.0}Cu_{0.46}Cd_{0.42}Ni_{0.33}Co_{0.020}$$

This ratio, except Co, agrees well with the mean elemental quota of $(N_{16}P_1)_{1000}Zn_{0.8}Cu_{0.38}Cd_{0.21}Co_{0.19}$ for 15 species of phytoplankton (including hard parts) grown in nutrient replete cultures (Ho et al., 2003). The 10-fold discrepancy in Co may result from differences in phytoplankton species or from a high concentration of Co (total 50 nM) in the culture medium. A consumption ratio of $(Si_{27}N_{16}P_1)_{1000}Zn_{1.0}Cu_{0.4}Cd_{0.05}Ni_{0.6}$ was observed in the Fe patch during SEEDS I (Kinugasa et al., 2005). This ratio is higher in Si and lower in Cd compared with that observed for this study. The two-fold discrepancy in Si may be due to a massive increase in fast-growing centric diatom (*Chaetoceros debilis*; ~20 $\mu g\,L^{-1}$ of chlorophyll-*a*) during SEEDS I. The reason for the eight-fold discrepancy in Cd is not clear.

The elemental ratios were different between the +Fe and control bottles (Table 6). The Si/P ratio in the control bottles (26 mol mol^{-1}) was approximately twice as high as that in the +Fe bottles (13 mol mol^{-1}). Takeda (1998) demonstrated that the Si/P ratio in phytoplankton collected from the subarctic North Pacific Ocean decreased from 31±7 mol mol^{-1} in the control bottles to 14±6 mol mol^{-1} in the Fe-added bottles. The good agreement suggests that Fe acts as a factor not only limiting the growth of phytoplankton, but also controlling the elemental stoichiometry of Si/P in marine phytoplankton.

Interestingly, the change in elemental ratio was also observed for Zn/P and Cd/P. The Zn/P ratio decreased from 1.7±0.2 mmol mol^{-1} in the control bottles to 1.0±0.1 mmol mol^{-1} in the +Fe bottles. The Cd/P ratio also decreased from 0.66±0.03 mmol mol^{-1} in the control bottles to 0.42±0.02 mmol mol^{-1} in the +Fe bottles. A similar change in Cd/P ratio has been reported in a culture of *Phaeodactylum tricornutum* (Kudo et al., 1996). They observed that cellular Cd/P ratio decreased with increasing growth rate. It resulted from the increase in cellular P contents, whereas the Cd content was almost constant. On the other hand, Cullen et al. (2003) performed bottle incubation of natural phytoplankton assemblages in the Southern Ocean with Fe addition (Fe concentrations: 0.2, 0.5, 1.0, 2.5 nM). After 10.7 days' incubation, they found the climax community being dominated by large diatoms (*Fragillariopsis*, *Pseudo-nitzschia*, and *Nitzschia*), and that Co/P, Zn/P and Cd/P ratios decreased from control values with increasing growth rate. The sampling locations are different between Cullen et al. (2003) and our study. Nevertheless, the changes in phytoplankton species and the decrease in Zn/P and Cd/P after Fe addition are comparable. These results indicate that Fe addition increases the growth rate and changes uptake stoichiometry, which results in the lower uptake ratios of Zn/P and Cd/P. Thus, Fe addition has implications for the biogeochemical cycling of Si, Zn and Cd.

The dissolved Pb was also transformed into the particulate species. Since the physiological requirement is not known for Pb, the transformation is probably a result of passive adsorption on biogenic particles. The Pb/P ratio in particulate matter was estimated to be 0.024 in the +Fe bottle.

5. Conclusions

Our data provide the temporal and spatial distributions of dissolved and particulate Co, Ni, Cu, Zn, Cd and Pb during the

mesoscale Fe enrichment in the western North Pacific. In addition, we conducted the bottle incubation with Fe addition (1 nM) using natural assemblages in the study area.

(1) Dissolved and total concentrations of trace metals before the Fe enrichment (day 0) were consistent with the reported data except for Co. Positive correlations between dissolved trace metals (Ni, Zn and Cd) and PO_4^{3-}, and between particulate trace metals (Ni, Zn and Cd) and chlorophyll-*a* were obtained, suggesting that biogeochemical cycling mainly controls the distributions of Ni, Zn and Cd.
(2) A bottle incubation experiment with Fe addition, in which mesozooplankton have been removed, showed a large increase in chlorophyll-*a* (up to 8.9 $\mu g L^{-1}$ for 10 days), suggesting that Fe deficiency was a factor limiting phytoplankton growth. As phytoplankton biomass increased, dissolved trace metals transformed into particulate species. Compared to the control bottles, lower elemental ratios of Si/P, Zn/P and Cd/P were observed, suggesting that Fe addition can affect the trace metal stoichiometry in marine phytoplankton.
(3) Mesoscale Fe enrichment showed increases in chlorophyll-*a* from 0.8 to 3.0 $\mu g L^{-1}$ on days 0–12. In the developing phases of the bloom, there was evidence of increasing concentrations in particulate Co, Ni, Cu and Cd, but no significant differences between concentrations inside and outside the patch. Dissolved trace metals also showed no significant differences between concentrations inside and outside the patch. Calculation using elemental ratios observed for the incubation and drawdown of PO_4^{3-} inside the patch indicates that no significant difference in particulate Co, Ni, Cu and Zn is reasonable because of the small increase in phytoplankton biomass and downward transport.
(4) Comparison of the bottle incubation and the mesoscale Fe enrichment suggests that grazing by mesozooplankton was also a significant factor controlling the phytoplankton biomass during the mesoscale Fe enrichment.

Acknowledgements

The authors thank to the chief scientist Atsushi Tsuda of The University of Tokyo, and the other scientists, officers and crew of the R/V *Hakuho Maru* and R/V *Kilo Moana* for their help with sampling. This work was supported by grants-in-aid for scientific research (Nos. 16204046 and 18710008) from the Ministry of Education, Culture, Sports, Science and Technology, Japan and by foundation of the Research Institute for Oceanochemistry. Finally,

Table A1
Concentrations of trace metals during the mesoscale Fe enrichment.

Depth (m)	Co (pM)		Ni (nM)		Cu (nM)		Zn (nM)		Cd (nM)		Pb (pM)	
	Par.	Dis.	Par.	Dis.	Par.	Dis.	Par.	Dis.	Par.	Dis.	Par.	Dis.
In day 0												
2	2.4	69	0.068	5.0	0.19	2.6	0.40	1.9	0.039	0.49	6.2	53
10	1.9	66	0.047	4.8	0.051	1.7	0.46	1.4	0.045	0.48	5.4	50
20	0.9	75	0.039	4.9	0.046	2.2	0.53	1.5	0.029	0.46	5.4	53
30	1.6	65	0.054	4.9	0.061	1.7	0.28	1.6	0.025	0.49	3.9	55
40	1.5	66	0.058	5.0	0.053	2.3	0.37	2.5	0.017	0.51	4.1	60
50	0.7	72	(0.11)	5.3	0.022	1.8	0.21	2.4	0.008	0.55	3.6	53
75	0.9	65	0.031	5.4	0.043	1.7	0.08	4.0	0.002	0.67	(7.3)	53
100	1.5	56	0.015	5.7	0.037	2.2	0.20	6.8	0.004	0.81	3.2	53
150	0.9	65	0.018	6.3	0.054	2.0	0.20	8.7	0.006	0.99	3.9	
In day 2												
5	2.3	70	0.056	5.3	0.19	2.8	0.51	1.7	0.052	0.50	7.9	54
10	NA[a]	68	NA	5.0	NA	1.8	NA	1.5	NA	0.47	NA	49
20	1.8	71	0.030	5.2	0.059	1.8	0.37	1.5	0.036	0.50	4.2	56
30	2.3	67	0.059	5.1	0.083	1.7	0.42	2.1	0.038	0.51	3.9	46
40	1.2	70	0.053	5.4	0.091	1.8	0.49	2.5	0.017	0.58	7.5	52
50	LD[b]	70	0.020	5.1	0.053	2.5	0.21	3.9	0.009	0.60	1.7	57
75	4.7	63	LD	5.3	0.080	1.9	0.23	3.5	0.007	0.62		53
100	1.3	53	LD	6.1	0.046	2.5	0.13	6.6	0.006	0.77	4.0	47
150	1.0	53	0.034	6.5	0.034	2.0	0.10	8.5	0.004	0.91	2.1	
In day 4												
5	3.0	66	0.058	5.0	0.23	3.2	0.68	1.8	0.063	0.43	6.1	50
10	2.5	70	0.049	5.1	0.15	2.6	0.50	(2.6)	0.043	0.43	3.3	57
20	2.2	67	0087	5.0	0.087	1.8	0.43	1.4	0.037	0.42	4.5	53
30	1.4	62	0.061	4.8	0.12	1.8	0.30	1.6	0.032	0.45	6.3	48
40	LD	67	0.025	4.8	0.084	2.2	0.18	3.2	0.012	0.50	2.5	69
50	LD	67	0.050	5.0	0.087	1.9	0.55	2.9	0.006	0.55	8.3	52
75	LD	66	LD	5.4	0.060	1.9	0.08	3.9	0.005	0.64	2.1	51
100	0.3	56	LD	5.9	0.052	1.8	0.08	6.4	0.003	0.82		46
150	0.6	51	0.022	6.5	0.053	2.2	0.08	8.7	0.003	0.96	2.0	52
In day 5												
5	3.2	65	0.071	4.9	0.213	2.5	(2.1)[c]	1.5	0.047	0.46	8.5	56
10	2.6	65	0.076	4.9	0.18	2.7	0.63	1.9	0.047	0.44	3.2	57
20	1.6	65	0.052	4.8	0.09	2.2	0.39	1.6	0.043	0.43	2.7	54
30	1.7	67	0.078	4.9	0.10	1.7	0.48	1.4	0.056	0.45	3.9	52
40	0.5	69	0.038	5.0	0.05	2.4	0.24	2.7	0.015	0.53	1.5	60
50	LD	70	0.029	5.3	0.04	2.0	0.15	3.1	0.009	0.56	1.5	
75	LD	64	LD	5.4	0.02	1.8	0.17	4.0	0.006	0.63	2.6	54
100	1.7	53	0.032	6.2	0.06	2.5	0.19	8.2	0.004	0.82	3.5	52
150	0.4	57	0.020	6.6	0.03	2 1	0.10	8.8	0.003	0.95	1.2	46

Tale A2
Concentrations of trace metals during the mesoscale Fe enrichment.

Depth (m)	Co (pM)		Ni (nM)		Cu (nM)		Zn (nM)		Cd (nM)		Pb (pM)	
	Par.	Dis.	Par.	Dis.	Par.	Dis.	Par.	Dis.	Par.	Dis.	Par.	Dis.
In day 7												
5	NA	62	NA	4.7	NA	2.0	NA	1.3	NA	0.46	NA	55
10	2.8	62	0.069	5.1	0.10	1.9	0.52	1.3	0.059	0.47	4.9	58
20	3.2	66	0.096	4.7	0.12	1.8	0.46	1.4	0.055	0.46	4.7	55
30	1.5	65	0.095	4.8	0.07	1.6	0.35	1.6	0.040	0.49	5.0	50
40	0.5	65	0.047	4.9	0.07	2.0	0.33	1.8	0.013	0.54	5.6	51
50	NA	67	NA	4.9	NA	1.6	NA	2.1	NA	0.57	NA	49
75	0.9	65	0.027	5.4	0.07	1.8	0.11	(11)	0.008	0.69	2.5	54
100	2.1	54	0.023	5.5	0.06	2.0	0.09	6.7	0.004	0.80	23	48
150	0.6	54	0.004	6.6	0.05	2.1	0.05	8.5	0.003	0.99	1.0	49
In day 8												
5	4.55	66	0.075	4.9	0.22	2.5	0.45	1.3	0.053	0.46	4.7	51
10	4.0	65	0.060	4.9	0.11	2.0	0.49	1.l	0.044	0.44	4.2	54
20	2.7	66	0.099	4.7	0.11	1.9	0.39	1.5	0.042	0.43	3.9	57
30	1.9	64	0.117	4.9	0.10	1.6	044	1.6	0.040	0.49	4.6	55
40	1.3	67	0.048	5.2	0.08	1.7	0.24	2.1	0.015	0.57	1.9	52
50	0.7	70	0.019	5.2	0.04	2.2	0.12	2.9	0.007	0.59	1.9	55
75	1.5	67	0.021	5.5	0.03	2.0	0.06	4.4	0.008	0.69	2.2	51
100	2.8	58	0.028	6.0	0.03	2.0	023	6.5	0.005	0.83	3.2	51
150	1.8	54	0.027	6.5	(0.22)	1.7	0.19	8.1	0.004	0.94	2.2	46
In day 10												
5	2.3	63	0.048	4.6	0.16	2.5	047	1.7	0.038	0.44	4.7	56
10	0.8	62	0.072	4.8	0.13	2.4	040	1.5	0.044	0.44	3.6	58
20	3.3	67	0.114	4.8	0.11	1.7	0.55	16	0.059	0.45	5.6	55
30	NA	NA									NA	NA
40	0.6	68	0.046	5.1	0.06	1.5	0.19	1.8	0.020	0.56	2.1	53
50	NA	74	NA	5.3	NA	1.9	NA	2.6	NA	0.61	NA	56
75	0.9	66	0.016	5.3	0.04	1.5	0.13	3.6	0.005	0.65	2.7	53
100	1.6	59	LD	5.7	0.03	2.0	0.06	6.7	0.008	0.79	2.6	47
150	0.5	56	LD	6.5	0.02	1.9	0.07	8.7	0.002	0.96	1.1	48
In day 11												
5	1.9	67	0.079	4.9	0.14	1.8	0.44	1.2	0.064	0.44	4.8	53
10	2.1	67	0.068	5.0	0.083	1.9	0.38	1.3	0.053	0.46	3.9	60
20	2.2	68	0.046	4.8	0.068	1.6	0.27	1.0	0.033	0.42	3.3	52
30	5.2	60	0.077	4.9	0.063	1.6	0.44	1.2	0.052	0.46	4.8	55
40	0.7	67	0.035	5.1	0.069	1.8	0.19	2.1	0.016	0.53	2.2	52
50	0.9	71	0.024	5.2	0.055	1.7	0.13	2.6	0.011	0.55	2.2	52
75	1.1	63	0.020	5.2	0.053	1.7	0.18	4.1	0.009	0.69	3.9	48
100	2.6	53	LD	5.7	0.037	2.2	0.23	6.6	0.006	0.83	2.9	47
150	1.4	54	LD	6.7	0.025	2.0	0.09	8.6	0.002	0.97	1.6	48

Table A3
Concentrations of trace metals during the mesoscale Fe enrichment.

Depth (m)	Co (pM)		Ni (nM)		Cu (nM)		Zn (nM)		Cd (nM)		Pb(pM)	
	Par.	Dis.	Par.	Dis.	Par.	Dis.	Par.	Dis.	Par.	Dis.	Pair.	Dis.
In day 12												
5	1.4	69	0.062	5.0	0.081	1.8	0.45	1.0	0.052	0.47	4.1	53
10	1.7	72	0.068	4.9	0.066	2.2	0.37	1.3	0.042	0.45	2.8	60
20	0.8	85	0.045	4.8	0.044	1.7	0.25	1.2	0.019	0.47	1.9	
30	1.5	63	0.081	4.7	0.056	1.4	0.27	1.1	0.035	0.47	2.5	51
40	LD	67	0.004	5.0	0.023	2.1	0.10	1.9	0.008	0.55	0.6	54
50	0.4	69	0.033	5.2	0.031	1.7	0.12	3.0	0.008	0.57	1.3	56
75	0.4	64	0.022	5.3	0.021	1.6	0.10	3.6	0.007	0.66	1.4	65
100	1.1	58	LD	5.5	0.024	1.9	0.13	5.6	0.006	0.72	1.7	49
150	1.0	NA	LD	NA	0.040	NA	0.24	NA	0.020	NA	1.4	NA
In day 13												
5		65		5.1		1.6		1.3		0.48		53
10		76		5.4		1.9		0.9		0.42		58
20		67		5.0		1.6		1.0		0.35		59
30		71		5.3		1.8		1.8		0.48		53
50		67		5.2		1.6		2.7		0.54		65
75		60		5.3		1.9		4.1		0.57		48

Table A3 (*continued*)

Depth (m)	Co (pM)		Ni (nM)		Cu (nM)		Zn (nM)		Cd (nM)		Pb(pM)	
	Par.	Dis.	Par.	Dis.	Par.	Dis.	Par.	Dis.	Par.	Dis.	Pair.	Dis.
In day 14												
5		61		4.9		1.7		2.1		0.43		54
10		66		4.9		1.8		1.9		0.41		57
20		72		5.0		1.7		2.0		0.36		56
30		68		5.0		1.5		4.7		0.41		50
50		65		5.2		1.4		6.2		0.53		53
75		71		5.5		1.8		5.4		0.59		50
In day 16												
5		69		5.0		1.6		0.9		0.39		55
10		80		5.1		1.8		1.1		0.41		59
20		72		5.0		1.7		1.3		0.39		60
30		76		5.3		1.8		3.0		0.46		55
50		80		5.5		2.0		3.4		0.54		57
75		82		5.8		2.1		5.2		0.59		53
In day 17												
5		64		4.9		1.5		2.2		0.34		56
10		64		4.9		1.5		1.4		0.34		56
20		65		4.9		1.8		1.8		0.32		56
30		65		5.0		1.5		2.5		0.41		52
50		67		5.3		1.6		3.6		0.51		53
75		67		5.4		1.7		4.3		0.52		51

Table A4
Concentrations of trace metals during the mesoscale Fe enrichment.

Depth (m)	Co (pM)		Ni (nM)		Cu (nM)		Zn (nM)		Cd (nM)		Pb (pM)	
	Par.	Dis.	Par.	Dis.	Par.	Dis.	Par.	Dis.	Par.	Dis.	Par.	Dis.
In day 19												
5		69		5.1		1.7		3.2		0.34		53
10		65		4.8		1.5		2.5		0.30		SI
20		66		4.8		1.9		2.5		0.34		53
30		60		4.8		1.4		1.9		0.37		50
50		60		4.9		1.4		3.2		0.43		49
75		66		5.1		1.6		4.2		0.49		46
In day 21												
5		67		4.9		1.7		1.2		0.34		52
10		69		5.0		1.7		0.8		0.35		56
20		67		4.7		1.6		1.1		0.34		50
50		65		4.7		1.6		1.9		0.38		49
50		72		5.3		1.7		2.8		0.48		51
75		69		5.4		1.8		4.7		0.52		50
In day 13												
5	1.0	62	0.040	4.8	0.21	3.5	0.36	1.4	0.035	0.36	3.9	54
10	1.4	65	0.029	5.0	0.074	2.2	0.20	1.2	0.023	0.36	1.8	56
20	1.3	64	0.032	5.1	0.068	15	0.27	0.9	0.034	0.34	(16)	56
30	1.2	65	0.011	5.0	0.069	2.3	0.32	2.6	0.034	0.37	15	68
40	0.9	65	0.029	4.7	0.070	1.4	0.28	1.5	0.024	0.45	3.1	94
50	0.7	77	LD	5.3	0.063	1.7	0.10	2.8	0.006	0.46	1.1	60
75	3.0	67	LD	5.2	0.065	2.3	0.13	5.0	0.010	0.56	2.9	72
100	2.2	65	LD	5.4	0.055	1.6	0.09	5.0	0.007	0.61	2.1	48
150	1.8	47	LD	6.0	0.071	1.7	0.25	8.5	0.003	0.79	(23)	53
In day 25												
5		66		4.8		2.4		1.6		0.4O		55
10		65		4.6		2.0		1.7		0.39		58
20		69		5.3		2.3		1.5		0.42		55
30		64		5.0		1.6		2.0		0.46		53
40		68		5.2		1.8		2.6		0.54		53
50		66		5.3		1.7		3.2		0.51		54
75		62		5.6		2.5		4.1		0.59		56
100		57		5.8		1.8		5.6		0.69		56
130		45		6.2		1.9		8.5		0.82		47

Table A5
Concentrations of trace metals during the mesoscale Fe enrichment.

Depth (m)	Co (pM)		Ni (nM)		Cu (nM)		Zn (nM)		Cd (nM)		Pb (pM)	
	Par.	Dis.	Par.	Dis.	Par.	Dis.	Par.	Dis.	Par.	Dis.	Par.	Dis.
Out day 2												
5	1.8	68	0.078	5.0	0.14	1.7	0.52	1.4	0.041	0.33	6.9	54
10	4.3	62	0.075	4.6	0.092	2.0	0.49	2.4	0.054	0.35	6.2	88
30	1.9	60	0.090	4.8	0.073	1.4	0.48	1.3	0.061	0.31	6.3	54
30	3.7	64	0.099	4.9	0.092	1.4	0.48	1.3	0.052	0.36	5.4	55
50	1.0	70	0.044	5.2	0.068	2.5	0.16	5.0	0.014	0.44	1.8	63
75	0.5	75	0.027	5.1	0.067	1.6	0.18	4.3	0.007	0.47	2.9	56
Out day 5												
5	2.8	67	0.051	5.1	0.14	2.3	0.45	(4.61)	0.046	0.40	4.2	59
10	2.9	62	0.074	5.1	0.12	2.4	0.95	1.8	0.049	0.38	6.1	53
20	2.6	68	0.061	5.1	0.08	1.7	0.53	(4.23)	0.043	0.41	4.6	60
30	3.3	71	0.049	5.1	0.08	1.8	0.42	1.3	0.048	0.40	4.1	46
50	1.0	69	0.039	5.0	0.07	2.2	0.20	2.3	0.018	0.43	2.9	45
75	1.2	63	LD	5.2	0.05	1.5	0.17	35	0.006	0.48	2.1	37
Out day 8												
5	4.3	65	0.078	5.0	0.12	1.9	0.44	1.4	0.061	0.39	5.1	47
10	3.7	65	0.074	5.2	0.08	2.7	0.38	2.3	0.058	0.42	4.4	53
20	3.0	74	0.082	5.1	0.03	1.5	0.35	1.7	0.049	0.38	5.2	59
30	3.5	60	0.087	5.2	0.06	1.6	0.30	1.6	0.039	0.39	3.3	46
50	0.7	71	0.037	5.2	0.04	2.2	0.09	6.5	0.012	0.49	2.1	55
75	1.2	64	LD	5.7	0.01	1.7	0.06	5.5	0.007	0.50	2.4	46
Out day 11												
5	1.6	63	0.037	5.0	0.048	1.9	0.46	1.1	0.048	0.34	(11)	45
10	1.9	59	0.049	5.1	0.054	7.2	0.43	0.9	0.051	0.34	3.7	47
20	4.2	72	0.082	5.1	0.080	2.0	0.61	1.6	0.067	0.33	5.4	49
30	1.0	66	0.049	5.6	0.054	1.3	0.44	4.7	0.042	0.37	5.8	48
50	LD	NA	LD	NA	0.043	NA	0.27	NA	0.015	NA	2.3	NA
75	LD	72	LD	5.7	0.026	2.0	0.19	3.3	0.008	0.48	3.0	48
Out day 18												
5		67		5.2		1.5		1.2		0.37		55
10		63		4.8		1.4		1.0		0.32		64
20		57		4.8		1.4		1.3		0.32		51
30		57		4.7		1.4		2.1		0.47		49
50		78		5.4		1.6		3.9		0.56		54
75		77		5.6		1.6		5.1		0.57		50

Table A6
Concentrations of trace metals during the mesoscale Fe enrichment.

Depth (m)	Co (pM)		Ni (nM)		Cu (nM)		Zn (nM)		Cd (nM)		Pb (pM)	
	Par.	Dis.	Par.	Dis.	Par.	Dis.	Par.	Dis.	Par.	Dis.	Par.	Dis.
Out day 24												
5	1.2	66	0.034	5.0	0.21	2.1	0.40	(4.0)	0.041	0.32	5.0	54
10	1.2	74	0.024	5.3	0.34	2.7	0.24	2.4	0.036	0.32	2.6	64
20	0.8	71		5.2	0.08	1.9	0.36	1.3	0.035	0.33	2.7	(122)
30	0.8	67	0.036	5.2	0.07	1.5	0.40	1.8	0.033	0.36	3.3	56
50	LD	69	LD	5.4	0.0?	2.5	0.20	4.6	0.010	0.45	1.3	60
75	LD	76	LD	5.6	0.04	1.7	0.14	4.6	0.007	0.46	2.1	68

[a]NA: not analyzed.[b]LD: lower than the detection limit.[c]Data in parentheses were ignored for the subsequent processing and discussion.

we appreciate the helpful comments from the two reviewers and editor (Mark Wells).

Appendix

All data on the dissolved and particulate trace metals during the mesoscale Fe enrichment are listed in Appendix tables, i.e. Tables A1–A6.

References

Abe, K., 2002. Preformed Cd and PO_4 and the relationship between the two elements in the northwestern Pacific and the Okhotsk Sea. Marine Chemistry 79, 27–36.

Aramaki, T., Nojiri, Y., Imai, K., 2009. Behavior of particulate materials during iron fertilization experiments in the Western Subarctic Pacific (SEEDS and SEEDS II). Deep-Sea Research II 56 (26), 2875–2888.

Banse, K., 1991. Rates of phytoplankton cell division in the field and in iron enrichment experiment. Limnology and Oceanography 36, 1986–1998.

Bruland, K.W., Orians, K.J., Cowen, J.P., 1994. Reactive trace metals in the stratified central North Pacific. Geochimica et Cosmochimica Acta 58, 3171–3182.

Coale, K.H., Johnson, K.S., Fitzwater, S.E., Gordon, R.M., Tanner, S., Chavez, F.P., Ferioli, L., Sakamoto, C.M., Rogers, P., Millero, F., Steinberg, P., Nightingale, P.D., Cooper, D.J., Cochlan, W.P., Landry, M.R., Constantinou, J., Rollwagen, G., Trasvina, A., Kudela, R., 1996. A massive phytoplankton bloom induced by an ecosystem-scale iron fertilization experiment in the equatorial Pacific Ocean. Nature 383, 495–501.

Coale, K.H., Johnson, K.S., Chavez, F.P., Buesseler, K.O., Barber, R.T., Brzezinski, M.A., Cochlan, W.P., Millero, F., Falkowski, P.G., Bauer, J.E., Wanninkhof, R.H., Kudela, R.M., Altabet, M.A., Hales, B.E., Takahashi, T., Landry, M.R., Bidigare, R.R., Wang, X., Chase, Z., Strutton, P.G., Friederich, G.E., Gorbunov, M.Y., Lance, V.P., Hilting, A.K., Hiscock, M.R., Demarest, M., Hiscock, W.T., Sullivan, K.F., Tanner, S.J., Gordon, R.M., Hunter, C.N., Elrod, V.A., Fitzwater, S.E., Jones, J.L., Tozzi, S., Koblizek, M., Roberts, A.E., Herndon, J., Brewster, J., Ladizinsky, N., Smith, G., Cooper, D.J., Timothy, D., Brown, S.L., Selph, K.E., Sheridan, C.C., Twining, B.S., Johnson, Z.I., 2004. Southern Ocean iron enrichment experiment: carbon cycling in high- and low Si waters. Science 304, 408–414.

Cullen, J.T., Lane, T.W., Morel, F.M.M., Sherrell, R.M., 1999. Modulation of cadmium uptake in phytoplankton by seawater CO_2 concentration. Nature 402, 165–167.

Cullen, J.T., Chase, Z., Coale, K.H., Fitzwater, S.E., Sherrell, R.M., 2003. Effect of iron limitation on the cadmium to phosphorus ratio of natural phytoplankton assemblages from the Southern Ocean. Limnology and Oceanography 48, 1079–1087.

da Silva, J.J.R.F., Williams, R.J.P., 2001. The Biological Chemistry of the Elements. Oxford University Press, New York.

Fujishima, Y., Ueda, K., Maruo, M., Nakayama, E., Tokutome, C., Hasegawa, H., Matsui, M., Sohrin, Y., 2001. Distribution of trace bioelements in the subarctic North Pacific Ocean and the Bering Sea (the R/V *Hakuho-Maru* Cruise KH-97-2). Journal of Oceanography 57, 261–273.

Frew, R., Bowie, A.R., Croot, P.L., Pickmere, S., 2001. Macronutrient and trace-metal geochemistry of an in situ iron-induced Southern Ocean bloom. Deep-Sea Research II 48, 2467–2481.

Gordon, R.M., Johnson, K.S., Coale, K.H., 1998. The behaviour of iron and other trace elements during the IronEx-I and PlumEx experiments in the Equatorial Pacific. Deep-Sea Research II 45, 995–1041.

Ho, T.-Y., Quigg, A., Finkle, Z.V., Milligan, A.J., Wyman, K., Flakowski, P.G., Morel, F.M.M., 2003. The elemental composition of some marine phytoplankton. Journal of Phycology 39, 1145–1159.

Kinugasa, M., Ishita, T., Sohrin, Y., Okamura, K., Takeda, S., Nishioka, J., Tsuda, A., 2005. Dynamics of trace metals during the subarctic Pacific iron experiment for ecosystem dynamics study (SEEDS2001). Progress in Oceanography 64, 129–147.

Kudo, I., Kokubun,, H., Matsunaga,, K., 1996. Chemical fractionation of phosphorus and cadmium in the marine diatom *Phaeodactylum tricornutum*. Marine Chemistry 52, 221–231.

Lacan, F., Francois, R., Ji, Y., Sherrell, R.M., 2006. Cadmium isotopic composition in the ocean. Geochimica et Cosmochimica Acta 70, 5104–5118.

La Fontaine, S., Quinn, J.M., Nakamoto, S.S., Page, M.D., Go?hre, V., Moseley, J.L., Kropat, J., Merchant, S., 2002. Copper-dependent iron assimilation pathway in the model photosynthetic eukaryote *Chlamydomonas reinhardtii*. Eukaryotic Cell 1, 736–757.

Lane, T.W., Saito, M.A., George, G.N., Pickering, I.J., Prince, R.C., Morel, F.M.M., 2005. A cadmium enzyme from a marine diatom. Nature 435, 42.

Martin, J.H., Coale, K.H., Johnson, K.S., Fitzwater, S.E., Gordon, R.M., Tanner, S.J., Hunter, C.N., Elrod, V.A., Nowicki, J.L., Coley, T.L., Barber, R.T., Lindley, S., Watson, A.J., Van Scoy, K., Law, C.S., Liddicoat, M.I., Ling, R., Stanton, T., Stockel, J., Collins, C., Anderson, A., Bidigare, R., Ondrusek, M., Latasa, M., Millero, F.J., Lee, K., Yao, W., Zhang, J.Z., Friederich, G., Sakamoto, C.M., Chavez, F., Buck, K., Kolber, Z., Greene, R., Falkowski, P., Chisholm, S.W., Hoge, F., Swift, R., Yungel, J., Turner, N.W., Nightingale, P.D., Hatton, A., Liss, P., Tindale, N.W., 1994. Testing the iron hypothesis in ecosystems of the equatorial Pacific Ocean. Nature 371, 123–129.

Moffett, J.W., Dupont, C., 2007. Cu complexation by organic ligands in the sub-arctic NW Pacific and Bering Sea. Deep Sea Research I 54, 586–595.

Morel, F.M.M., Price, N.M., 2003. The biogeochemical cycles of trace metals in the oceans. Science 300, 944–947.

Nakatsuka, S., Okamura, K., Norisuye, K., Sohrin, Y., 2007. Simultaneous determination of suspended particulate trace metals (Co, Ni, Cu, Zn, Cd and Pb) in seawater with small volume filtration assisted by microwave digestion and flow injection inductively coupled plasma mass spectrometer. Analytica Chimica Acta 594, 52–60.

Nishioka, J, Takeda, S., Kondo, Y., Obata, H., Doi, T., Tsumune, D., Wong, C.S., Johnson, W.K., Sutherland, N., Tsuda, A., 2009. Changes in iron concentrations and bio-availability during an open-ocean mesoscale iron enrichment in the western subarctic Pacific, SEEDS II, Deep-Sea Research II 56 (26), 2796–2809.

Noriki, S., Arashitani, M., Minakawa, M., Harada, K., Tsunogai, S., 1998. vertical cycling of Cu and Ni in the western North and Equatrial Pacific. Marine Chemistry 59, 211–218.

Peers, G., Price, N.M., 2006. Copper-containing plastocyanin used for electron transport by an oceanic diatom. Nature 441, 341–345.

Quigg, A., Finkel, Z.V., Irwin, A.J., Rosenthal, Y., Ho, T.-Y., Reinfelder, J.R., Schofield, O., Morel, F.M.M., Falkowski, P.G., 2003. The evolutionary inheritance of elemental stoichiometry in marine phytoplankton. Nature 425, 291–294.

Saito, H., Tsuda, A., Nojiri, Y., Aramaki, T., Ogawa, H., Yoshimura, T., Imai, K., Kudo, I., Nishioka, J., Ono, T., Suzuki, K., Takeda, S., 2009. Biogeochemical cycling of N and Si during the mesoscale iron-enrichment experiment in the western subarctic Pacific (SEEDS-II), Deep-Sea Research II 56 (26), 2852–2862.

Saito, M.A., Moffett, J.W., Chisholm, S.W., Waterbury, J.B., 2002. Cobalt limitation and uptake in prochlorococcus. Limnology and Oceanography 47, 1629–1636.

Suzuki, R., Ishimaru, T., 1990. An improved method for the determination of phytoplankton chlorophyll using N,N-dimethylformamide. Journal of Oceanography 46, 190–194.

Takeda, S., 1998. Influence of iron availability on nutrient consumption ratio of diatoms in oceanic waters. Nature 393, 774–777.

Tsuda, A., Takeda, S., Saito, H., Nishioka, J., Nojiri, Y., Kudo, I., Kiyosawa, H., Shiomoto, A., Imai, K., Ono, T., Shimamoto, A., Tsumune, D., Yoshimura, T., Aono, T., Hinuma, A., Kinugasa, M., Suzuki, K., Sohrin, Y., Noiri, Y., Tani, H., Deguchi, Y., Tsurushima, N., Ogawa, H., Fukami, K., Kuma, K., Saino, T., 2003. A mesoscale iron enrichment in the western subarctic Pacific induces a large centric diatom bloom. Science 300, 958–961.

Tsuda, A., Takeda, S., Saito, H., Nishioka, J., Kudo, I., Nojiri, Y., Suzuki, K., Uematsu, M., Wells, M.L., Tsumune, D., Yoshimura, T., Aono, T., Aramaki, T., Cochlan, W.P., Hayakwa, M., Iwai, K., Isada, T., Iwamoto, Y., Johnson, W.K., Kameyama, S., Kato, S., Kiyosawa, H., Kondo, Y., Levasseur, M., Machida, R.J., Nagao, I., Nakagawa, F., Nakanishi, T., Nakatsuka, S., Narita, A., Noiri, Y., Obata, H., Ogawa, H., Oguma, K., Ono, T., Sakuragi, T., Sasagawa, M., Sato, M., Shimamoto, A., Takata, H., Trick, C.G., Watanabe, Y.W., Wong, C.S., Yoshie, N., 2007. Evidence for the grazing hypothesis: grazing reduces phytoplankton responses of the HNLC ecosystem to iron enrichment in the Western Subarctic Pacific (SEEDS II). Journal of Oceanography 63, 983–994.

Tsuda, A., Saito, H., Machida, R.J., Shimode, S., 2009. Meso- and microzooplankton responses to an *in situ* iron fertilization experiment (SEEDS II) in the northwest subarctic Pacific. Deep-Sea Research II 56 (26), 2767–2778.

Twining, B.S., Baines, S.B., Fisher, N.S., 2004. Element stoichiometries of individual plankton cells collected during the Southern Ocean iron experiment (SOFeX). Limnology and Oceanography 49, 2115–2128.